AD-A038 889 STEVENS INST OF TECH HOBOKEN N J DAVIDSON LAB F/G 13/10
A STUDY OF THE FEASIBILITY OF WAVE PULSE TECHNIQUES FOR EXPERIM--ETC(U)
DEC 76 J F DALZELL N00014-76-C-0348
UNCLASSIFIED SIT-DL-76-C-1928 NL

1 OF 1
AD A038889

END
DATE FILMED
5-77

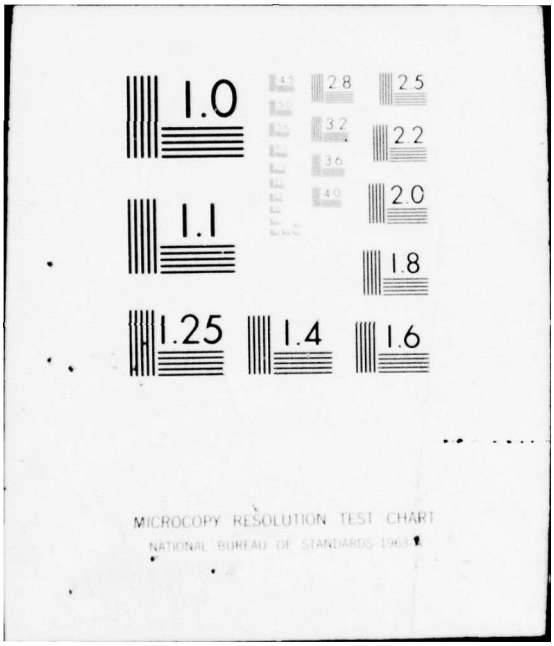
1.0
1.1
1.25
1.4
1.6
1.8
2.0
2.2
2.5
2.8
3.2
3.6
4.0
MICROCOPY RESOLUTION TEST CHART
NATIONAL BUREAU OF STANDARDS 1963

AD A038889

STEVENS INSTITUTE OF TECHNOLOGY

CASTLE POINT STATION
HOBOKEN, NEW JERSEY 07030

R-1928

DDC
RECEIVED
APR 29 1977

DAVIDSON LABORATORY

Report SIT-DL-76-1928

A STUDY OF THE FEASIBILITY OF WAVE PULSE TECHNIQUES FOR EXPERIMENTAL DETERMINATION OF ADDED RESISTANCE

by

J.F. Dalzell

December 1976

Final Report
1 October 1975 to 31 December 1976

APPROVED FOR PUBLIC RELEASE;
DISTRIBUTION UNLIMITED

Prepared for
David Taylor Naval Ship Research
and Development Center (1505)
Bethesda, Maryland 20084

Office of Naval Research
800 N. Quincy Street
Arlington, Virginia 22217

R-1928

UNCLASSIFIED

SECURITY CLASSIFICATION OF THIS PAGE (When Data Entered)

REPORT DOCUMENTATION PAGE	READ INSTRUCTIONS BEFORE COMPLETING FORM
1. REPORT NUMBER: SIT-DL-76-1928	2. GOVT ACCESSION NO. / 3. RECIPIENT'S CATALOG NUMBER (9)
4. TITLE (and Subtitle): A STUDY OF THE FEASIBILITY OF WAVE PULSE TECHNIQUES FOR EXPERIMENTAL DETERMINATION OF ADDED RESISTANCE (6) (14)	5. TYPE OF REPORT & PERIOD COVERED: FINAL rept. 1 Oct 1975 — 31 Dec 1976 (13)
	6. PERFORMING ORG. REPORT NUMBER: SIT-DL-76-1928
7. AUTHOR(s): J.F. Dalzell (10)	8. CONTRACT OR GRANT NUMBER(s): N00014-76-C-0348 (15) new
9. PERFORMING ORGANIZATION NAME AND ADDRESS: Davidson Laboratory, Stevens Institute of Technology, Castle Point Station, Hoboken, NJ 07030	10. PROGRAM ELEMENT, PROJECT, TASK AREA & WORK UNIT NUMBERS: SR 023 01 01
11. CONTROLLING OFFICE NAME AND ADDRESS: David Taylor Naval Ship Research and Development Center, Bethesda, MD 20084 (11)	12. REPORT DATE: December 1976 / 13. NUMBER OF PAGES: ii + 69 pages
14. MONITORING AGENCY NAME & ADDRESS (if different from Controlling Office): Office of Naval Research, 800 N. Quincy Street, Arlington, VA 22217 (12) 73p.	15. SECURITY CLASS. (of this report): UNCLASSIFIED / 15a. DECLASSIFICATION/DOWNGRADING SCHEDULE
16. DISTRIBUTION STATEMENT (of this Report): APPROVED FOR PUBLIC RELEASE; DISTRIBUTION UNLIMITED (16) SR0230101 (17) SR023010101	
17. DISTRIBUTION STATEMENT (of the abstract entered in Block 20, if different from Report)	
18. SUPPLEMENTARY NOTES: Sponsored by the Naval Sea Systems Command, General Hydromechanics Research Program--administered by the David Taylor Naval Ship Research and Development Center, Code 1505, Bethesda, MD 20084	
19. KEY WORDS (Continue on reverse side if necessary and identify by block number): GHR Program; Added Resistance, Functional Series, Wave Pulse	

20. ABSTRACT (Continue on reverse side if necessary and identify by block number)

Because the experimental determination of the characteristics of mean ship model resistance added by waves is one of the more difficult and time consuming problems in seakeeping towing tank practice, it was of practical interest to see if a technique involving wave pulses could be developed, and if so, if it promised better efficiency. Toward this end a fairly realistic digital simulation was made of the wave pulse experiment and of the resulting resistance transient. The analysis of the problem was approached from the

next page

DD FORM 1 JAN 73 1473 EDITION OF 1 NOV 65 IS OBSOLETE S/N 0102-014-6601

104 750

UNCLASSIFIED

SECURITY CLASSIFICATION OF THIS PAGE (When Data Entered)

20. point of view that in order to be practically attractive, any resulting technique must involve a very few wave pulse runs, preferably only one. In the event, no conceptually clear approach to the analysis of a single resistance transient could be found. By taking advantage of the general properties of the quadratic model which appears to be valid for added resistance, it was possible to develop a "dirty" approach for the identification of the mean added resistance operator from a single transient experiment. However, no useful results could be obtained with this latter approach. It appears that there is not really enough information in a single resistance transient to enable even the identification of the mean added resistance operator. It also appears that if there is a practical wave pulse technique for added resistance experiments it is not yet in hand.

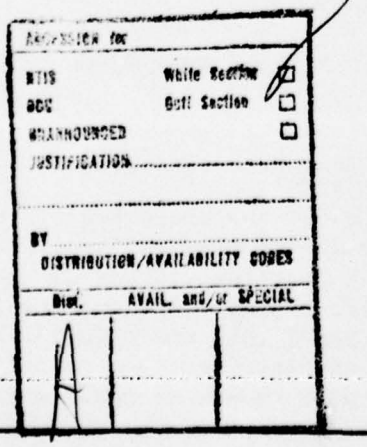

STEVENS INSTITUTE OF TECHNOLOGY
DAVIDSON LABORATORY
CASTLE POINT STATION
HOBOKEN, NEW JERSEY

REPORT SIT-DL-76-1928

December 1976

A STUDY OF THE FEASIBILITY OF WAVE PULSE TECHNIQUES FOR EXPERIMENTAL DETERMINATION OF ADDED RESISTANCE

by

J.F. Dalzell

This research was carried out under the
Naval Sea Systems Command
General Hydromechanics Research Program
SR 023-01-01 administered by the
David Taylor Naval Ship Research and Development Center
under Contract N00014-76-C-0348

(DL Project 4358/184)

APPROVED FOR PUBLIC RELEASE; DISTRIBUTION UNLIMITED

Reproduction in whole or in part is permitted
for any purpose of the United States Government.

Approved

Daniel Savitsky
Deputy Director

CONTENTS

INTRODUCTION

The work summarized in Ref. 1* has shown that a functional polynomial input-output model has considerable practical promise as a unifying concept for the interpretation of ship added resistance and possibly related problems. In particular, in this and previous work it has been demonstrated that; a) both a linear and a quadratic frequency response function can be derived from experiments in irregular waves, as well as from experiments in regular waves; b) synthesis of the mean added resistance and of resistance spectra can be carried out by use of these frequency response functions, and; c) time histories of added resistance can be synthesized for an irregular wave input through use of the time domain representation of the linear and quadratic level non-linear frequency response functions.

All of the just cited work was empirical. The particular input-output model was hypothesized at the outset and the implications of the model were checked as far as possible with experiment. The idea that there exist linear and quadratic frequency response functions followed from the (non-physical) model assumed. The input-output model provides no detailed physical basis. In the context of added resistance, a linear frequency response function may be thought of as the relation between oscillatory surge exciting force and wave elevation. There are a number of hydromechanical approaches to the estimation of this function so that the concept could be accepted as having an identifiable physical base. On the other hand, methods of hydromechanical computation for the entire quadratic response function were lacking. Only a very special portion of the quadratic frequency response function could be estimated from hydromechanical considerations. This problem was addressed in the work

---

*1. Dalzell, J.F., "Application of the Functional Polynomial Model to the Ship Added Resistance Problem," Eleventh Symposium on Naval Hydrodynamics, London, March 1976.

of Ref. 2*, and in this latter work the relationship between the hydromechanics of added resistance and the "quadratic frequency response function" of the input-output model was clarified. Reasonably good qualitative, and fair quantitative agreement was achieved between results of analysis and experiment. Thus the work of Ref. 2, by providing a physical model, lends increased confidence to the use of the two-term functional polynomial model in analysis and interpretation of experiment.

Insofar as ship model dynamics in waves is concerned, the general experimental problem is to identify the pertinent parameters or functions given a wave input and the observed response. An input-output model of some sort is ordinarily required if an endless series of experiments is to be avoided.

Historically, the advent of the linear input-output model for some ship dynamics problems had the effect of expanding the possibilities in experimental ship dynamics work. Once it was shown that the linear model was a reasonable engineering approach for the prediction of ship response under realistic (random) conditions, three experimental techniques were admissible. Regular wave experiments took on a slightly different meaning, the option became available for the interpretation of experiments in irregular waves by spectral analysis, and the development of transient test techniques[3*] followed shortly thereafter. Of the three techniques the first two are the most widely used, although the transient technique has undergone additional development in recent years, Takezawa, et al[4,5*].

---

*2. Dalzell, J.F. and Kim, C.H., "Analytical Investigation of the Quadratic Frequency Response for Added Resistance," SIT-DL-76-1878, Davidson Laboratory, Stevens Institute of Technology, August 1976.

3. Davis, M.C. and Zarnick, E.E., "Testing Ship Models in Transient Waves," Fifth Symposium on Naval Hydrodynamics, Bergen, 1964.

4. Takezawa, S. and Takekawa, M., "Advanced Experimental Techniques for Testing Ship Models in Transient Water Waves: Part I, The Transient Test Technique on Ship Motions in Waves," Eleventh Symposium on Naval Hydrodynamics, London, 1976.

5. Takezawa, S. and Hirayama, T., "Advanced Experimental Techniques for Testing Ship Models in Transient Water Waves: Part II, The Controlled Transient Water Waves for Using in Ship Motion Tests," Eleventh Symposium on Naval Hydrodynamics, London, 1976.

Given this history and the evidence thus far advanced that the two term functional polynomial is a realistic input-output model for added resistance, it is natural to inquire into the extent to which techniques paralleling the three available for the linear case are available for routine experimental determination of the quadratic frequency response function.

A regular wave technique has been used for some time in the determination of mean added resistance operators. In this technique the total mean resistance of a model in regular waves is measured and the added resistance operator is derived from the difference between this observation and the model resistance in calm water. Multiple runs are required to cover a range of wave frequency and it has been found by some that frequent re-running of calm water tests is advisable. Many of the basic problems with the technique appear to be related to experimental accuracy. The mean added resistance is usually small in comparison with calm water resistance, and both are often very small in comparison with the time dependent component.

Because the mean added resistance operator corresponds only to a special portion of the quadratic frequency response function, the existing regular wave technique is not sufficient if experimental estimates of the entire function are required. The principle of the required regular wave technique has been indicated in Reference 1. However, this technique has not so far been used in practice. In brief, to produce results defining the entire quadratic response function for added resistance, an experimental technique involving dual harmonic excitation is required; that is, two superimposed regular waves. This technique corresponds to the basic interpretation of the quadratic frequency response function given in Ref. 1. It would involve selection of pairs of regular wave frequencies such that their superposition in the encounter domain is periodic, as well as the subsequent harmonic analysis of the added resistance response. The general nature of the quadratic frequency response function and the principle of the regular wave technique imply that if N experimental runs in regular waves are adequate to describe the important part of the added resistance operator, then about $N^2/2$ runs might be required for a reasonable definition

of the entire function. Thus a 10 run per model speed mean added resistance test program might turn into a 50 run per speed program for the general quadratic response.

With respect to the possibilities of identifying the linear and the quadratic frequency response functions from data obtained in irregular waves, the techniques are more or less available. Ordinary spectral and cross-spectral analyses suffice for the linear function, and a technique called cross-bi-spectral analysis has been developed for the quadratic function (Ref.1). In principle the cross-bi-spectral analysis technique is quite attractive in the sense of increasing efficiency over that for regular wave experiments. The technique is based on a correlation with the wave fluctuations of the fluctuations in resistance. Thus this technique is not sensitive to the value of calm water resistance, and in fact calm water resistance need not be known at all. Again in principle, either the mean added resistance or the entire quadratic frequency response may be derived from the same sample of irregular wave input and response, the difference being the amount of computer time brought to bear. In practice however, the technique has a quite serious deficiency. It is that for reasonable precision of estimates an order of magnitude larger sample is presently required than is customary in the spectral identification of the linear response. In many cases it is not possible to accumulate sufficient sample for the linear identification process in one pass up a towing tank. Thus it appears that the cross-bi-spectral analysis technique will always require as many or more test runs as the existing regular wave technique if only the mean added resistance operator is required -- although fewer for a determination of the entire function. The mean added resistance operator is presently the only part of the quadratic frequency response function which finds routine use, and it is to be expected that the situation will not soon materially change. Accordingly, it does not now appear that the technique involving cross-bi-spectral analysis of irregular wave test data will offer savings in facility time over that now required for routine added resistance experiments.

In parallel with the possibilities for the linear case, the third experimental technique involves the analysis of transient wave pulses.

Conceptually, the transient wave pulse would involve all wave frequencies of interest, and the wave elevation would be zero or nearly so at beginning and end of experiment. Thus the observed resistance transient, while containing response at all frequencies, should equal calm water resistance at beginning and end of the experiment. The ideal advantages are thus similar to those for the cross-bi-spectral analysis technique in that all the required information is embedded somehow in a single observation. The difficulty with the idea is essentially that the existing theory for the quadratic input-output model does not contain a clear indication of how to proceed with the analysis.

It was accordingly the objective of the present work to investigate the feasibility of a wave pulse technique for added resistance. For the practical reasons cited previously the emphasis was to be upon identification of the mean added resistance operator rather than the entire quadratic frequency response function, and the methods to be employed were to involve digital computer rather than physical experiments.

THE TRANSIENT EXPERIMENT

In order to fix some terminology, various stages of the hypothetical transient experiment for head seas are outlined in Figure 1. In the figure the condition of tank and model are indicated for five significant stages of one experimental run. Time (t) will be considered to be positive after the wave generator is started. Thus there is shown at the top of the figure for $t < 0$ a hypothetical towing tank which has a wave generator at one end, an absorber at the opposite end, and a model sitting still in preparation for the run. At this stage the water is assumed to be quiet everywhere. Position in the tank is denoted by X, which is zero at the wavemaker and positive in the direction of wave propagation.

At time equal to zero the wave generator begins to generate a long-crested transient wave, and typically at some subsequent time the model acceleration begins so that at the second stage ($t=t_s$) the model is proceeding with constant velocity, U, at tank position $X=X_s$. The model is assumed to be in still water at this stage while the wave transient at the other end of the tank is propagating toward it. In the third stage ($t=t_{st}$) the model enters the wave pulse at tank position $X=X_{st}$. At the fourth stage ($t=t_{et}$) the model leaves the pulse at position X_{et}, and continues at constant speed in calm water until time t_e (position X_e) when deceleration begins. The useful part of the experiment is between times t_s and t_e, during which an observer on the model sees calm, then rough, and then finally calm water at the end. Because of the assumption of constant speed, the position of the model in the tank is known during this time from a knowledge of X_s, t_s and U.

Several of the tacit assumptions in the above deserve comment. One is that of a long-crested wave pulse or transient. The input-output model has not been extended to the short-crested case. For the purposes of the present study this is not a serious restriction since none of the other techniques described in the introduction have been adapted for this case, and in fact there have as of the present been very few experiments of any type in short-crested seas.

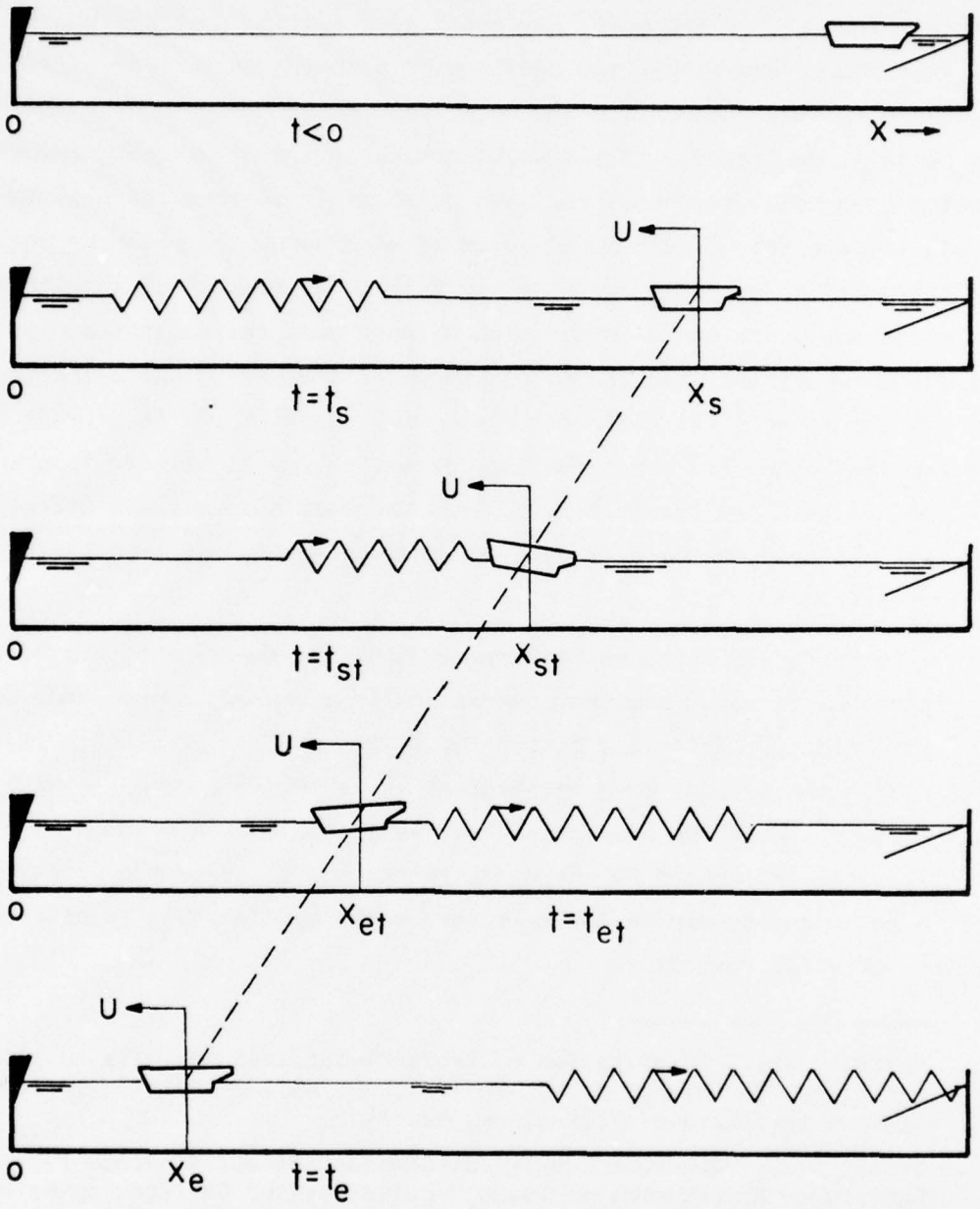

FIGURE 1 EVENTS IN THE HEAD SEA TRANSIENT EXPERIMENT

Another comment which can be made is about the subject of heading. Clearly, if there is some component of wave group velocity in the direction of model travel there may be an ambiguity which would require very special handling, or the model may never pass out of the transient at all -- at least not within the confines of a towing tank. For example, in following seas the model might be started near the wave maker before the pulse is generated. If all wave components travel at group velocity greater than model velocity, the wave pulse will overtake and pass the model. Alternately if the model speed is high enough it might be possible for the model to overtake and pass the pulse. In between these extremes it is extremely difficult to envision a reasonable following seas transient experiment when the model speed and the mean group velocity of the wave components are about the same. For purposes of the present study the problems about all model headings excepting head seas were ignored on the grounds that the feasibility of even the head sea test was not clear, and that the head sea case is usually considered the most important for added resistance.

The assumption of constant model velocity implies that the model is restrained in surge and that resistance is measured through some sort of force balance. This is a system not always used in practice. It was retained in the present case because; a) it is feasible to do[6*]; b) it has been found[7,8*] that the mean added resistance for constant speed is not significantly influenced by surge restraint; and c) it seemed probable that a technique developed for this case might be adaptable to other conditions of surge restraint.

---

*6. Dalzell, J.F., "Application of Cross-Bi-Spectral Analysis to Ship Resistance in Waves," SIT-DL-72-1606, AD 749102, Davidson Laboratory, Stevens Institute of Technology, May 1972.

7. Sibul, O.J., "Constant Thrust vs. Constant Velocity Method for Resistance Measurement in Waves," University of California, Berkeley, Report NA-71-1, June 1971.

8. Journee, J.M.J., "Motions, Resistance and Propulsion of a Ship in Longitudinal Regular Waves," Report 428, Laboratorium voor Sheepshydromechanica, Technische Hogeschool Delft, May 1976.

WAVE PULSES

Theory

It was the basic objective of the work to examine feasibility of techniques which might be employed in towing tanks, and to check any promising scheme with a computer "experiment." Accordingly it was necessary to begin with a consideration of the type of wave transient which is physically possible, and to generate a few examples for later use. References 3 and 5 indicate clearly that because of the dispersive properties of waves, it is not possible to produce anything closely resembling the ideal impulse, or the isolated step function, etc., which are basic to much of the theory of transient response as shown in the textbooks of control and electronics.

The linear theory of the type of wave pulse which is possible is well developed, is treated in References 3 and 5, and will be used herein. It is apparent from these references that the linear theory and experiment correlate well so long as average local wave steepnesses are not such as to produce extensive breaking.

Following the developments in References 3 and 5, the transient wave elevation at position X in the tank will be denoted $h_x(t)$. It is assumed that $h_x(t)$ is absolutely integrable, that is:

$$\int | h_x(t) | dt < \infty$$

where the convention is followed that omission of limits signifies limits of plus and minus infinity. (This convention will be followed throughout the present report.) On the basis of this assumption, the transient has a Fourier transform or complex spectrum, $H_x(\omega)$, and the transform pair relating the transient and its spectrum may be defined as:

$$h_x(t) = \frac{1}{2\pi} \int H_x(\underline{\omega}) \, \mathrm{Exp}[\, i\underline{\omega}t \,] d\underline{\omega} \tag{1}$$

$$H_x(\underline{\omega}) = \int h_x(t) \, \mathrm{Exp}[\, -i\underline{\omega}t \,] dt \tag{2}$$

where $\underline{\omega}$ denotes circular wave frequency.

In the practical production of a wave transient, the wavemaker is given a specified sequence of control signals so as to produce a desired transient wave elevation. For present purposes the dynamics of the wavemaker may be neglected and it will be assumed that the transient wave at the wavemaker is specified. Thus the wave at X=0 (Figure 1) will be taken to be:

$$h_o(t) = \frac{1}{2\pi} \int H_o(\underline{\omega}) \, \mathrm{Exp}[\, i\underline{\omega}t \,] d\underline{\omega} \tag{3}$$

where

$H_o(\underline{\omega})$ is the complex spectrum of the wave pulse.

There are two main constraints on $h_o(t)$. The first is that it be zero for $t < 0$; that is, $h_o(t)$ must be physically realizable according to the time conventions shown in Figure 1. The second is that the local wave steepnesses be "small."

Following the linear theory of wave propagation[3,5], the frequency response function connecting the wave elevation at X=0 (Eq.3) and wave elevation elsewhere in the tank is given by:

$$\mathrm{Exp}[\, -i \mid \underline{\omega} \mid \underline{\omega} X/g \,]$$

which simply means that each wave component is assumed to propagate without change in amplitude. From this, the spectrum of the wave transient at position X becomes:

$$H_x(\underline{\omega}) = H_o(\underline{\omega}) \, \mathrm{Exp}[\, -i \mid \underline{\omega} \mid \underline{\omega} X/g \,] \tag{4}$$

and the transient wave itself at position X is:

$$h_x(t) = \frac{1}{2\pi} \int H_o(\underline{\omega}) \, \mathrm{Exp}[\, i\underline{\omega}t - i \mid \underline{\omega} \mid \underline{\omega} X/g \,] d\underline{\omega} \tag{5}$$

Also following from the linear assumption is that the integral square of the transient is invariant with tank position:

$$E_x = \int h_x^2(t)\,dt = \frac{1}{2\pi}\int |H_o(\underline{\omega})|^2\, d\underline{\omega} = \text{constant} \tag{6}$$

in which the last relation is obtained by application of the Parseval Theorem.

The invariance of the integral square suggests a useful change in notation for the complex spectrum of the transient at the wavemaker:

$$H_o(\underline{\omega}) = A(\underline{\omega})\,\mathrm{Exp}[i\varphi(\underline{\omega})] \tag{7}$$

in which $A(\underline{\omega})$ and $\varphi(\underline{\omega})$ are real
and:

$$A(-\underline{\omega}) = A(\underline{\omega})$$

$$\varphi(-\underline{\omega}) = -\varphi(\underline{\omega})$$

Then the wave transient at position X becomes:

$$h_x(t) = \frac{1}{2\pi}\int A(\underline{\omega})\,\mathrm{Exp}[i\underline{\omega}t + i\varphi(\underline{\omega}) - i\,|\underline{\omega}|\,\underline{\omega}X/g]\,d\underline{\omega} \tag{8}$$

In the transient techniques described in References 3,4,5 the amplitude part of the spectrum of the wave at the wavemaker, $A(\underline{\omega})$, is specified so as to produce wave excitation in all the frequencies of interest. The phase part, $\varphi(\underline{\omega})$, is used to control the wave pulse in the run area.

It is shown in Reference 5 that the wave pulse of shortest duration has a constant phase spectrum. Accordingly, for the shortest duration of pulse, it is necessary to specify a part of $\varphi(\underline{\omega})$ so that the $|\underline{\omega}|\,\underline{\omega}X/g$ term in Eq. (8) is cancelled out at the position of interest. Thus the phase function for the transient at the wavemaker may be specified as follows:

$$\varphi(\underline{\omega}) = C\pi\,\mathrm{sgn}(\underline{\omega}) + |\underline{\omega}|\,\underline{\omega}X_m/g - \underline{\omega}t_m \tag{9}$$

In Eq. (9) C is an arbitrary constant. The second term is a phase lead which will cancel the similar phase lag in Eq. (8) at position X_m. The last term is a phase lag which corresponds to a constant time delay in the time domain. It must be included in the phase prescription as a way

to insure that the transient at the wavemaker will be physically realizable. What is accomplished by the above assumption is to organize the transient wave at the wavemaker in such a way that about an equal time is necessary for all component waves to reach position X_m in the tank. At positions closer to the wavemaker the transient pulse is converging, and at positions further away than X_m the transient is diverging.

In practical testing in the usual towing tank a desirable mid-point of the data taking portion of the run is usually known from the acceleration and deceleration characteristics of the carriage drive, and from the positions of the inevitable obstructions at either end of the tank. Thus the tank position, X_m, in Eq. (9) might reasonably be specified as the mid-point of the data run, and would ordinarily be determined by other than wave making considerations. In the terminology of Figure 1:

$$X_m = (X_s + X_e)/2 \tag{10}$$

Thus substituting Eq. (9) into Eq. (8) there results a further expression for the wave pulse at any tank position X:

$$\begin{aligned} h_x(t) &= \frac{1}{2\pi} \int A(\underline{\omega}) \mathrm{Exp}[\, i\underline{\omega}\,(t-t_m) + iC\pi \mathrm{sgn}(\underline{\omega}) - i\,|\,\underline{\omega}\,|\,\underline{\omega}(X-X_m)/g]\, d\underline{\omega} \\ &= \frac{1}{\pi} \int_0^\infty A(\underline{\omega}) \cos[\underline{\omega}(t-t_m) + C\pi - \underline{\omega}^2 (X-X_m)/g]\, d\underline{\omega} \\ &= \frac{1}{\pi} \int_0^\infty A(\underline{\omega}) \cos[C\pi - \underline{\omega}t_m - \underline{\omega}^2 (X-X_m)/g] \cos\underline{\omega}t \; d\underline{\omega} \\ &\quad - \frac{1}{\pi} \int_0^\infty A(\underline{\omega}) \sin[C\pi - \underline{\omega}t_m - \underline{\omega}^2 (X-X_m)/g] \sin\underline{\omega}t \; d\underline{\omega} \end{aligned} \tag{11}$$

In the present case the encountered wave transient, $h_e(t)$, is desired. It may be assumed that timing of model acceleration relative to wavemaker start can be made such that the model will arrive at position X_m at time $(t_m - \delta)$. For constant model velocity, U, the position of the model in the tank may then be written as:

$$X = X_m - U(t - t_m + \delta) \tag{12}$$

In the practical case Eq. (12) is valid only within the range of time

($t_s \leq t \leq t_e$). Now substituting Eq. (12) into Eq. (11) there results an expression for the encountered transient:

$$h_e(\tau+t_m) = \frac{1}{2\pi} \int B(\underline{\omega}) \exp[i\tau(\underline{\omega} + |\underline{\omega}|\underline{\omega}U/g)]d\underline{\omega} \tag{13}$$

where: $\tau = t - t_m$

$$B(\underline{\omega}) = B_R(\underline{\omega}) + iB_I(\underline{\omega})$$

with:

$$B_R(\underline{\omega}) = A(\underline{\omega})\cos[C\pi sgn(\underline{\omega}) + |\underline{\omega}|\underline{\omega}U\delta/g]$$

$$B_I(\underline{\omega}) = A(\underline{\omega})\sin[C\pi sgn(\underline{\omega}) + |\underline{\omega}|\underline{\omega}U\delta/g] \tag{14}$$

With respect to the practical experiment, Eq. (13) is valid only in the range $(t_s - t_m) \leq \tau \leq (t_e - t_m)$. The time variable change corresponds to the normal practice in experiments of counting time with reference to some arbitrary point in the constant speed portion of the run. The function $B(\underline{\omega})$ contains only parameters which are prescribed by programming of the wave machine, and the timing of model start. The function of $\underline{\omega}$ in the exponential of Eq. (13) may be recognized as the encounter frequency for head seas, ω. The expression, Eq. (13), may thus be transformed into an integration over ω. As such it is in the form of a Fourier Transform. So long as matters are arranged so that $h_e(t)$ is zero outside the range of practical validity of Eq. (13), the inverse transform of the encountered transient will be valid in the sense that there will be no difference between the practical experiment and the hypothetical situation in which the model proceeds at constant velocity for an infinite range of τ.

Applying the head sea transformation:

$$\omega = \underline{\omega} + |\underline{\omega}|\underline{\omega}U/g$$

and defining:

$$K(\omega) = \frac{g}{2U}\left(-1 + \sqrt{1+4\omega U/g}\right)$$

$$J(\omega) = 1/\sqrt{1+4\omega U/g} \tag{15}$$

$$h_e(\tau+t_m) = \frac{1}{\pi}\int_0^\infty B_R(K(\omega))J(\omega)\cos(\omega\tau)\,d\omega$$

$$- \frac{1}{\pi}\int_0^\infty B_I(K(\omega))J(\omega)\sin(\omega\tau)\,d\omega \qquad (16)$$

The effective Fourier spectrum of the encountered transient is $B(K(\omega))J(\omega)$. From Eq. (14):

$$|\,B(K(\omega))J(\omega)\,| = A(K(\omega))J(\omega) \qquad (17)$$

so that, as would be expected, the amplitude part of the Fourier spectrum is distorted by the transformation.

Example Evaluations

As noted, some examples of physically possible wave pulses were desired. The easiest way to insure realism was to evaluate Eq. (11) with parameters appropriate to a given tank and model size. The Davidson Laboratory Tank No. 3 (300'x12'x6') was selected as the hypothetical tank, and the hypothetical experiment was assumed to involve a five foot ship model at a speed corresponding to Froude Number 0.15.

The first function to specify is $A(\underline{\omega})$. It was assumed on the basis of prior experimental results[6] that wave lengths between 2.5 and 15 feet (1/2 to 3 times model length) would include the important parts of the resistance response. It was further assumed that for the identification purposes envisioned it would be of advantage to make the encountered spectrum have a roughly constant modulus (Eq.17) in the encounter frequency range which corresponds to the wave length range just cited. The first step in constructing $A(\underline{\omega})$ was thus to make $A(\underline{\omega}) = A(K(\omega)) = P/J(\omega)$ where P is a constant which controls the magnitude of the generated transient. The model speed assumed in computing encounter frequencies corresponded to a Froude Number of 0.15 for a five foot model. The resulting form for $A(\underline{\omega})$ is shown in Figure 2. The wave frequency range of interest was roughly 3.5 to 9 radians/second. In this range the function is as noted above. At each end of this range a smooth transition is made to zero over a one radian/second frequency range.

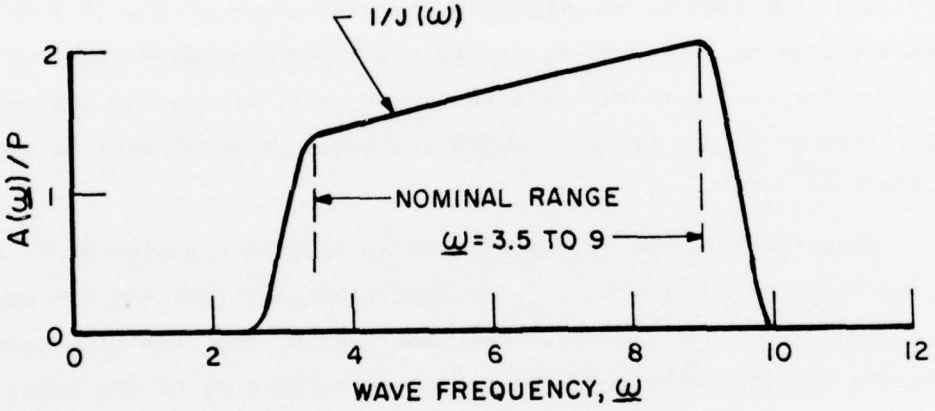

FIGURE 2 FORM OF SPECIFIED MODULUS OF SPECTRUM OF WAVEMAKER TRANSIENT FOR FROUDE NUMBER 0.15

The next parameters required by Eq. (11) are X_m and t_m. In D.L. Tank 3 the mid-point of the data taking area is usually 150 feet from the wavemaker, and this distance was chosen for X_m, the designed concentration point. The time delay was chosen to be a bit more than the time required for the wave component of highest frequency to travel 150 feet at its group velocity. The number used was t_m = 105 seconds.

The constant, C, in Eq. (11) controls the symmetry of the wave transient at the point of maximum concentration. If the constant is made zero, the concentrated transient will tend to have a higher maximum crest than maximum trough. If the constant is ± 0.5 the maximum crests and troughs are the same. For present purposes a value of -0.5 was taken.

All that remains to choose in the evaluation of Eq. (11) is the arbitrary scaling constant, P, in the specified wavemaker spectrum modulus. This constant is essentially the wavemaker gain, and may be assigned any number from zero to a value at which the waves produced will be too steep and start to break.

Equation (11) was evaluated with an arbitrary choice of P, and the parameters selected previously, for four tank positions (at the wavemaker, and at 125, 150 and 175 feet). The magnitude of the resulting wave amplitudes was compared with the wave length corresponding to the local apparent periods to establish a reasonable maximum value of P.

Figure 3 shows the resulting computed transients scaled to correspond to the estimated maximum amplitude. As required, the wave pulse at the wavemaker is zero for time less than zero. The time duration of the pulse decreases with position in the tank until the 150 foot position, whereafter the duration increases. The transient at the point of concentration (150') appears small in the figure because the vertical scale is less than half of that for the other positions. The maximum peak to peak amplitude shown for the 150 foot position is about 0.5 feet, which is probably equivalent to a wave height to wave length ratio of 1/10. At the 125 and 175 foot positions maximum apparent local steepness appears to be about 1/18, and at the wavemaker maximum apparent local steepness is less than 1/20. For these reasons the wave pulses shown in Figure 3 were taken as representing a practical possibility for a relatively severe wave pulse.

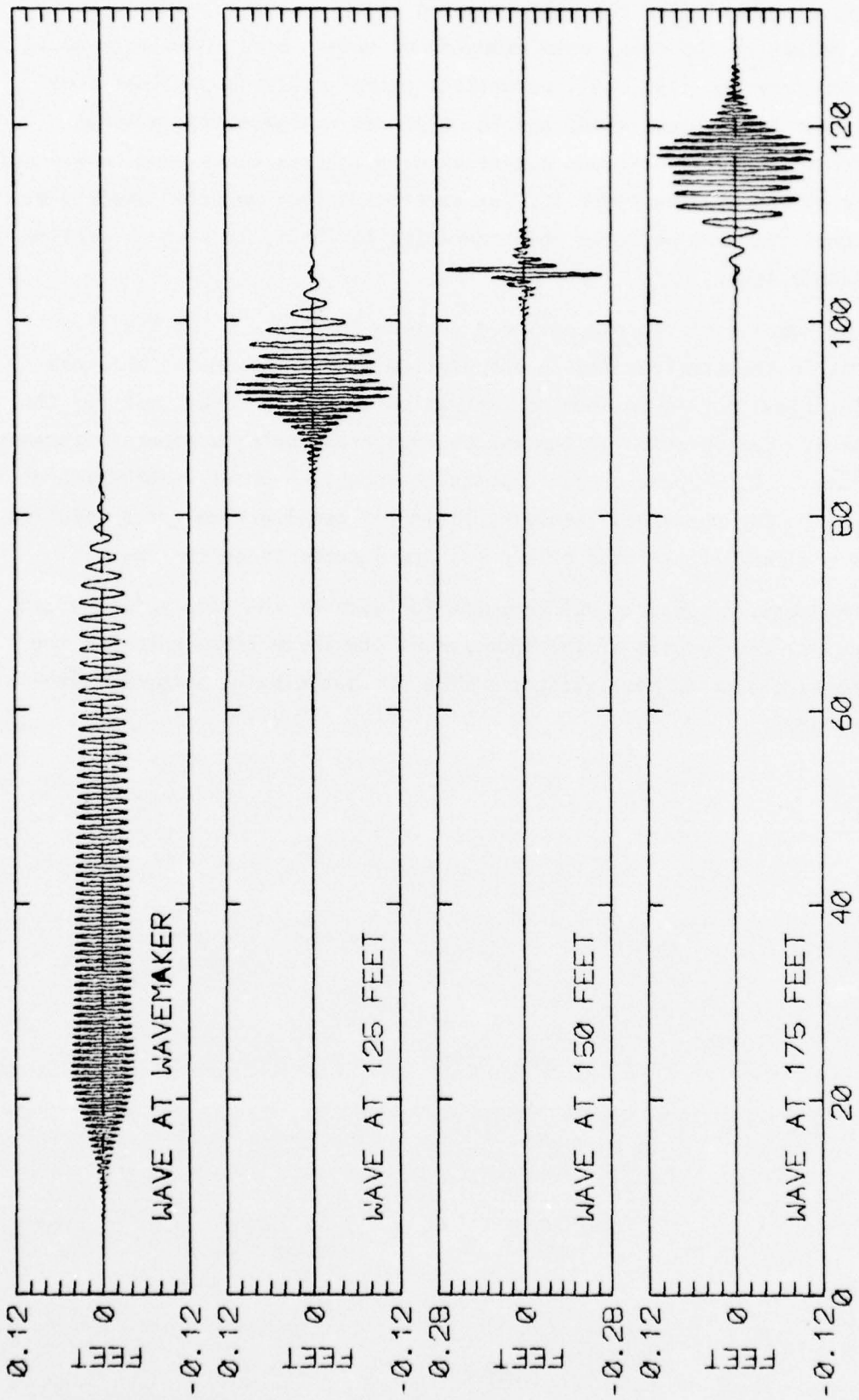

FIGURE 3 COMPUTED WAVE TRANSIENTS OF MAXIMUM AMPLITUDE AT FOUR TANK POSITIONS

Having established that the computed results were reasonable for specific points in the tank, some examples of encountered transients could be computed from Eq. (13). All parameters except the model arrival time delay, δ, had been established, and Eq. (13) was evaluated for a model speed corresponding to a Froude Number of 0.15. Three cases were considered according to whether the model arrives at the 150 foot position exactly at time t_m when the wave pulse is most concentrated (δ=0), 10 seconds earlier, or 10 seconds later.

The results of the evaluation are shown in Figure 4 for the three cases. As in the previous figure the vertical scale chosen for the case of model arrival during maximum concentration is smaller than that for the other cases. The duration of the encountered transients is about 10 seconds in all cases. This duration corresponds to roughly 4 model lengths travel up the tank. For the speed involved, timing of model arrival at a specific point in the tank within plus or minus a few seconds is quite feasible.

The complex spectrum was computed for each of the wave pulses shown in Figure 4. The modulus of the spectrum of the three transients was the same, and as expected, was constant within the anticipated encounter frequency range.

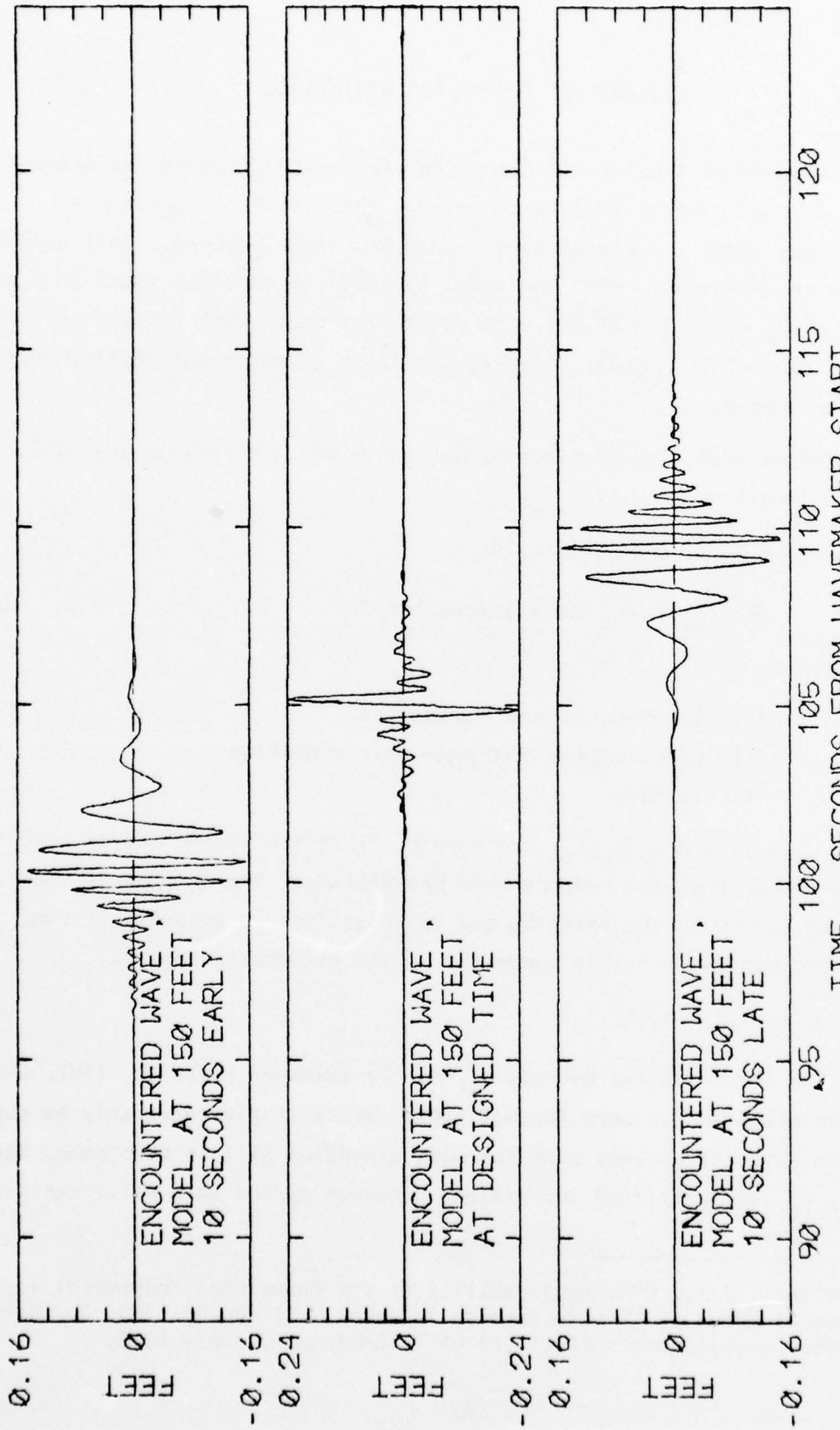

FIGURE 4 COMPUTED ENCOUNTERED WAVE PULSES OF MAXIMUM AMPLITUDE (FROUDE NUMBER 0.15)

INPUT-OUTPUT THEORY FOR RESISTANCE

As noted in the introduction, the basic assumption in the present work is that ship model resistance follows the functional polynomial input-output model treated in Refs. 1,2,6,9*, and elsewhere. This approach involves the assumption that the model proceeds at constant speed in a wave system, h(t), which is defined at a point stationary with respect to the mean position of the model; that is, the input-output model applies to the encounter domain.

The general time domain representation for the resistance, r(t), is written as follows:

$$r(t) = g_o + \int g_1(t_1)h(t-t_1)dt_1 + \iint g_2(t_1,t_2)h(t-t_1)h(t-t_2)dt_1 dt_2 \qquad (18)$$

where:

- r(t) is instantaneous resistance
- h(t) represents a zero mean wave elevation
- t is time

and g_o, $g_1(t_1)$, and $g_2(t_1,t_2)$ are zeroth, first and second degree kernels. It is presumed that the hydrodynamic properties of the ship model are contained wholly in the kernels, and (without loss in generality) that the second degree kernel is symmetric in its arguments; that is,

$$g_2(t_2,t_1) = g_2(t_1,t_2)$$

The zeroth degree kernel, g_o, is the value of r(t), Eq. (18), when the wave elevation is zero for all time. Since it may reasonably be supposed on physical grounds that the wave elevation will be zero mean, the kernel, g_o, is identified for present purposes as the calm water resistance.

---

*9. Dalzell, J.F., "The Applicability of the Functional Polynomial Input-Output Model to Ship Resistance in Waves," SIT-DL-75-1794, Davidson Laboratory, Stevens Institute of Technology, January 1975.

The second term in Eq. (18) is a linear convolution integral and is interpreted as the oscillatory surge exciting force so that the first degree kernel is the impulse response function for surge force.

The third term in Eq. (18) is a double convolution integral which gives rise to the essentially non-linear resistance added by waves. The second degree kernel may be called a quadratic impulse response.

Both first and second degree kernels are assumed to be absolutely integrable and thus may be transformed in the Fourier sense. The transform pairs relating the linear and quadratic impulse responses to corresponding linear and quadratic frequency response functions may be defined as follows:

$$g_1(\tau) = \frac{1}{2\pi} \int e^{+i\omega\tau} G_1(\omega)\, d\omega$$

$$G_1(\omega) = \int e^{-i\omega\tau} g_1(\tau)\, d\tau \tag{19}$$

$$g_2(\tau_1,\tau_2) = \frac{1}{(2\pi)^2} \iint \mathrm{Exp}\left[+i\omega_1\tau_1 + i\omega_2\tau_2\right] G_2(\omega_1,\omega_2)\, d\omega_1\, d\omega_2$$

$$G_2(\omega_1,\omega_2) = \iint \mathrm{Exp}\left[-i\omega_1\tau_1 - i\omega_2\tau_2\right] g_2(\tau_1,\tau_2)\, d\tau_1\, d\tau_2 \tag{20}$$

in which ω represents circular encounter frequency.

The linear frequency response function, $G_1(\omega)$, defined by Eq. (19) is absolutely conventional.

The quadratic frequency response function, $G_2(\omega_1,\omega_2)$ is defined in a bi-frequency plane. Because the kernel $g_2(\tau_1,\tau_2)$ is assumed to be symmetrical in its arguments, and is real:

$$G_2(\omega_1,\omega_2) = G_2(\omega_2,\omega_1) \tag{21}$$

$$G_2^*(\omega_1,\omega_2) = G_2(-\omega_1,-\omega_2)$$

$$= G_2(-\omega_2,-\omega_1) \tag{22}$$

(The asterisk denotes the complex conjugate.) These relationships simplify the quadratic frequency response function to the extent that certain

symmetries result and that as a consequence the function needs only to be considered in a quadrant of the bi-frequency (ω_1, ω_2) plane. Equation (21) results in a line of symmetry along the line $\omega_2 = \omega_1$. Equation (22) results in a line of symmetry of the real part, and anti-symmetry of the imaginary part of $G_2(\omega_1, \omega_2)$ defined by $\omega_2 = -\omega_1$. (It may be noted that along this line the imaginary part of the function is zero.) These two lines and the ω_1, ω_2 axes divide the bi-frequency plane into octants, of which the two on either side of the positive ω_1 axis may be arbitrarily chosen for reference. The assumptions of symmetry of the second degree kernel results, with Eq. (20), in a complete definition of $G_2(\omega_1, \omega_2)$ if the functions are defined in any pair of octants including a semi-axis of either frequency. Thus without loss in generality, interpretation of the quadratic frequency response needs only to involve the octants on either side of the positive ω_1 axis. In these octants ω_1 is positive and $|\omega_1| \geq |\omega_2|$.

Because estimates of the quadratic frequency response function are the objective of the present work, a summary (after Ref.1) of the interpretation of the function is in order. The approach to the meaning of the function is grossly the same as for the linear case. If in the linear case the system is considered to be excited by

$$h(t) = a \cos\omega t$$

the output may then be written:

$$\mathrm{Re}\{aG_1(\omega)\,\mathrm{Exp}(i\omega t)\}$$

and $G_1(\omega)$ is interpreted in terms of normalized amplitude and phase of response.

To interpret the quadratic frequency response, <u>dual</u> harmonic excitation is necessary. Accordingly, it may be assumed that:

$$h(t) = a_1 \cos\omega_1 t + a_2 \cos\omega_2 t \qquad (23)$$

In accordance with the previous discussion of symmetry, both frequencies (ω_1, ω_2) are considered positive and $|\omega_1| \geq |\omega_2|$. The basic model, Eq. (18) is good for any zero-mean excitation. Accordingly, Eq. (23) may be

substituted directly in Eq. (18). After some algebra the final result for the response to dual harmonic excitation may be written as follows:

$$
\begin{aligned}
r_2 = {} & g_o \\
& + \mathrm{Re}\{a_1 G_1(\omega_1)\,\mathrm{Exp}(i\omega_1 t) + a_2 G_1(\omega_2)\,\mathrm{Exp}(i\omega_2 t)\} \\
& + \tfrac{1}{2}\{a_1^2 G_2(\omega_1,-\omega_1) + a_2^2 G_2(\omega_2,-\omega_2)\} \\
& + \tfrac{1}{2}\,\mathrm{Re}\{a_1^2 G_2(\omega_1,\omega_1)\,\mathrm{Exp}(i2\omega_1 t)\} \\
& + \tfrac{1}{2}\,\mathrm{Re}\{a_2^2 G_2(\omega_2,\omega_2)\,\mathrm{Exp}(i2\omega_2 t)\} \\
& + \mathrm{Re}\{a_1 a_2 G_2(\omega_1,\omega_2)\,\mathrm{Exp}[i(\omega_1+\omega_2)t]\} \\
& + \mathrm{Re}\{a_1 a_2 G_2(\omega_1,-\omega_2)\,\mathrm{Exp}[i(\omega_1-\omega_2)t]\} \qquad (24)
\end{aligned}
$$

This result shows that the response of the quadratic system, Eq. (18), to dual excitation contains, in general, a shift in the mean and components of six different frequencies [ω_1, ω_2, $2\omega_1$, $2\omega_2$, $(\omega_1+\omega_2)$, and $(\omega_1-\omega_2)$]. The second and third terms of the result are the superposition of the linear responses at the excitation frequencies. The fourth and fifth terms of Eq. (24) represent a shift in the mean. These terms allow the identification of the mean added resistance operator as the value of $G_2(\omega_1,\omega_2)$ along the line $\omega_2=-\omega_1$ (or $G_2(\omega_1,-\omega_1)$). The sixth and seventh terms are the second harmonic components $(2\omega_1, 2\omega_2)$. Similarly, these terms allow the identification of second harmonic response with the values of $G_2(\omega_1,\omega_2)$ along the line $\omega_2=\omega_1$ (or $G_2(\omega_1,\omega_1)$).

The eighth and ninth terms of Eq. (24) pertain to the bi-frequency plane in general. The eighth term is the response at frequency $(\omega_1+\omega_2)$; that is, $G_2(\omega_1,\omega_2)$ expresses the normalized response in the sum frequency due to non-linear interactions. Similarly, the ninth term involves response at frequency $(\omega_1-\omega_2)$; that is, $G_2(\omega_1,-\omega_2)$ is the normalized response in the difference frequency.

A final part of the general theory which is useful in both analysis and interpretation is the effect of cascaded linear systems. If it is supposed that the input to the system, h(t) of Eq. (18) is the result of

a linear operation upon a variable s(t), and the frequency response function of the linear operation is denoted by $L_1(\omega)$, then the linear and quadratic frequency response functions ($K_1(\omega)$ and $K_2(\omega_1,\omega_2)$) connecting s(t) and r(t) may be written:

$$K_1(\omega) = G_1(\omega) L_1(\omega) \tag{25}$$

$$K_2(\omega_1,\omega_2) = G_2(\omega_1,\omega_2) L_1(\omega_1) L_1(\omega_2) \tag{26}$$

If it is additionally supposed that the output r(t) of the system of Eq. (18) acts upon a linear system with frequency response function $L_2(\omega)$ to produce an output v(t), then the linear and quadratic frequency response functions ($K_1^{SV}(\omega)$ and $K_2^{SV}(\omega_1,\omega_2)$) connecting s(t) and v(t) may be written:

$$K_1^{SV}(\omega) = G_1(\omega) L_1(\omega) L_2(\omega) \tag{27}$$

$$K_2^{SV}(\omega_1,\omega_2) = G_2(\omega_1,\omega_2) L_1(\omega_1) L_1(\omega_2) L_2(\omega_1+\omega_2) \tag{28}$$

The relation for the linear part, Eq. (27), is just the same as for completely linear systems.

Equation (28) shows that filtering of input and output have different effects on the apparent frequency response function. For example, if $L_1(\omega)$ is an ideal low-pass filter with cutoff frequency α, the effective quadratic frequency response function, $K_2^{SV}(\omega_1,\omega_2)$, will be zero outside the region where $|\omega_1|$ and $|\omega_2|$ are less than α. Considering a practical example of output filtering, if the output is observed through a low-pass filter, $L_2(\omega)$, with a very low frequency cutoff, the effective quadratic frequency response will tend to be zero everywhere except near the line $\omega_2=-\omega_1$ which is the location of the mean added resistance operator in the bi-frequency plane.

SIMULATION OF RESISTANCE TRANSIENTS

General

Following the conditions involved in the simulation of encountered wave pulses, Figure 4, it was assumed that the simulated experiment involved a five foot ship model proceeding at a Froude Number of 0.15 into a head wave pulse. In order to take advantage of quantitative resistance response data developed in Refs, 2, 6 and 9, the model was assumed to be the Series 60 0.60 block parent, restrained in surge. Because it is customary in a narrow towing tank to locate a wave probe ahead of the model to minimize distortion of results by model generated waves, the encountered wave pulses, Figure 4, were assumed to be the indication of a wave probe one model length forward of model LCG.

The simulated wave pulses are digital time series; that is, represent a sampling of the wave pulse at a uniform time interval (Δt). Accordingly the analytical time domain model, Eq. (18), has to be re-cast into a summation form for practical computation purposes. This was done in the same way as had been done in Ref. 9. The digital model of Eq. (18) becomes:

$$r(n) = g_o + \sum_{j=-ml}^{m2} L_j\, h(n-j) + \sum_{j=-pl}^{p2}\sum_{k=-pl}^{p2} Q_{jk}\, h(n-j)h(n-k) \qquad (29)$$

where $r(n)$ = computed resistance time series

$h(n)$ = simulated wave pulse time series

and L_j and Q_{jk} are weighting coefficients in which the differentials are absorbed.

Equation (29) requires discrete approximations to the linear and quadratic impulse responses of the form:

$$\bar{g}_1(\tau) = L_j \, \delta(\tau - j\Delta t) \tag{30}$$

$$\bar{g}_2(\tau_1, \tau_2) = Q_{jk} \, \delta(\tau_1 - j\Delta t)\delta(\tau_2 - k\Delta t) \tag{31}$$

(where $\delta(t)$ is the Dirac delta function)

The Fourier transforms of Eqs. (30) and (31) in accordance with Eqs. (19) and (20) yield continuous (aliased) frequency response functions as follows:

$$\bar{G}_1(\omega) = \sum_{j=-m1}^{m2} L_j[\cos(j\omega\Delta t) - i \sin(j\omega\Delta t)] \tag{32}$$

$$\bar{G}_2(\omega_1, \omega_2) = \sum_{j=-p1}^{p2} \sum_{k=-p1}^{p2} Q_{jk}[\cos(j\omega_1\Delta t + k\omega_2\Delta t) - i \sin(j\omega_1\Delta t + k\omega_2\Delta t)] \tag{33}$$

For practical computing purposes the process of transforming given observed or analytical frequency response functions amounts to achieving (with a finite number of coefficients) a reasonable fit of the re-transformed impulse responses (Eqs. 32,33) to the observed response functions. The general approach followed is to integrate the first of Eqs. (19) and (20) trapezoidally with observed estimates of the appropriate frequency response function. This is carried out for a sufficient range of time variable(s) so that decisions regarding the truncation limits (m1, m2, and p1, p2 in Eqs. 29 through 33) can be made. Evaluation of the computed impulse response function is made at integer values of time step Δt and these values are multiplied by Δt or Δt^2 as appropriate to result in estimates of the coefficients L_j and Q_{jk}. The next step is to adjust the coefficients so that the discrete kernel reflects the correct behavior of the frequency response functions at zero frequency. In the present case it is assumed that there is no resistance added by an infinitely long wave. Thus the coefficients L_j and Q_{jk} should sum to zero. The final computational step is to insert the coefficients into Eqs. (32) or (33), compute the re-transformed impulse response function and compare the results with the original frequency response estimates. Iteration of the process is sometimes necessary.

Selection of Data for Use in Eq. (29)

To take advantage of the results of Refs. 2, 6 and 9, it was convenient to retain the non-dimensionalizations of those references. The first convention is that all lengths are divided by model length. For present purposes this meant only that the simulated wave pulse elevations were to be divided by five feet. The second convention was that model resistance was to be divided by model displacement. Finally, a non-dimensional encounter frequency was defined as:

$$\sigma = \omega/\omega_{1L}$$

where ω = encounter frequency, rad/sec

ω_{1L} = frequency of a wave of model length, L

$= \sqrt{2\pi g/L}$

Because this non-dimensionalization can be considered as merely a change in the time scale, the σ notation of Refs. 2, 6 and 9 may be used interchangeably with the present ω notation. For present purposes the time scale will be multiplied by ω_{1L} and corresponding frequencies computed in the conventional way. In particular, the real time sampling interval (Δt) of the wave pulses of Figure 4 was selected to be 0.066 seconds. The equivalent Δt in the "non-dimensional" time scale is 0.4197, and this value was used through the developments of the weighting coefficients in Eqs. (29) through (33) to be described.

The first term in Eq. (29) is the calm water resistance, g_o. The experimental value of raw calm water resistance cited in Ref. 6 for the five foot series 60 model at a Froude Number of 0.15 was 0.092 lb. Dividing this by model displacement yields:

$$g_o = 0.0028$$

The second term in Eq. (29) involves the linear weighting coefficients L_j. Several sets of estimates from experiment had been made in Ref. 6 for the modulus of the surge exciting force frequency response function, $G_1(\omega)$ or $G_1(\sigma)$. These were averaged to form a starting point for the derivation. The phase data was not presented in Ref. 6, but

had been developed. These phase estimates had been derived with respect to wave elevation forward of LCG. This wave reference had been shifted in time to improve the cross-spectral estimation procedure, and it was a straightforward operation to correct the estimates to a wave phase reference one model length ahead of model LCG.

The operations described in conjunction with Eqs. (30) through (33) were carried out upon the experimental surge exciting force data and the results are summarized in Figures 5 and 6. Figure 5 indicates the experimental estimates of the surge exciting force frequency response function as plus signs, and the results of re-transforming the final weighting coefficients, L_k, as dashed lines. As may be noted, the experimental data which was thought valid in Ref. 6 does not cover the entire frequency range. (Extrapolations had been made to zero and high frequency before starting the transformation procedure.) However the encounter frequency range of the example wave pulses does not significantly exceed the frequency range where data is shown, and it would thus not be expected that the results of the simulation would be seriously influenced by errors in the extrapolations. Overall, the correspondence between the transformed discrete linear kernal and the experimental data appears adequate to insure realism in the simulation.

The weighting coefficients, L_k, in Figure 6 are of most importance for positive k; that is, for the "past" of the input wave elevation. Accordingly the kernel relating surge exciting force to wave elevation a model length ahead of LCG is nearly physically realizable.

For a starting point for the simulation of the third term in Eq. (29) there were four choices available. Reference 9 contains three sets of experimental estimates of the quadratic frequency response function for the experimental case of interest, and Ref. 2 contains one set of analytical estimates. It appears from the analyses of Ref. 2 that in the regions of the bi-frequency plane not resolved in Ref. 9 there exist significant values of the quadratic frequency response function. Additionally, some of the experimental estimates which were questioned in Ref. 9 appear to have been discredited by the analyses of Ref. 2.

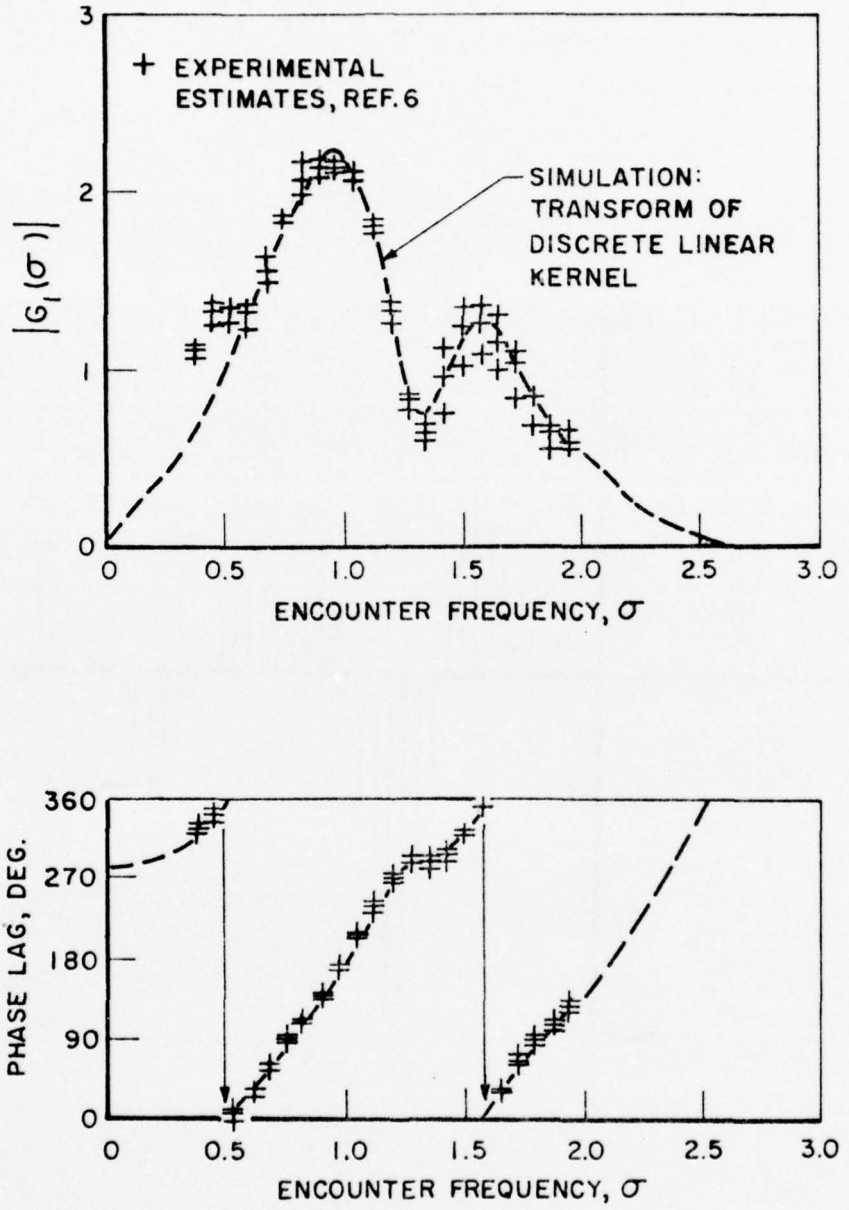

FIGURE 5 SURGE EXCITING FORCE FREQUENCY RESPONSE FUNCTION FOR SERIES 60, 0.60 BLOCK MODEL AT FROUDE NUMBER 0.15 (PHASES ARE REFERENCED TO WAVE ELEVATION ONE MODEL LENGTH FORWARD OF LCG)

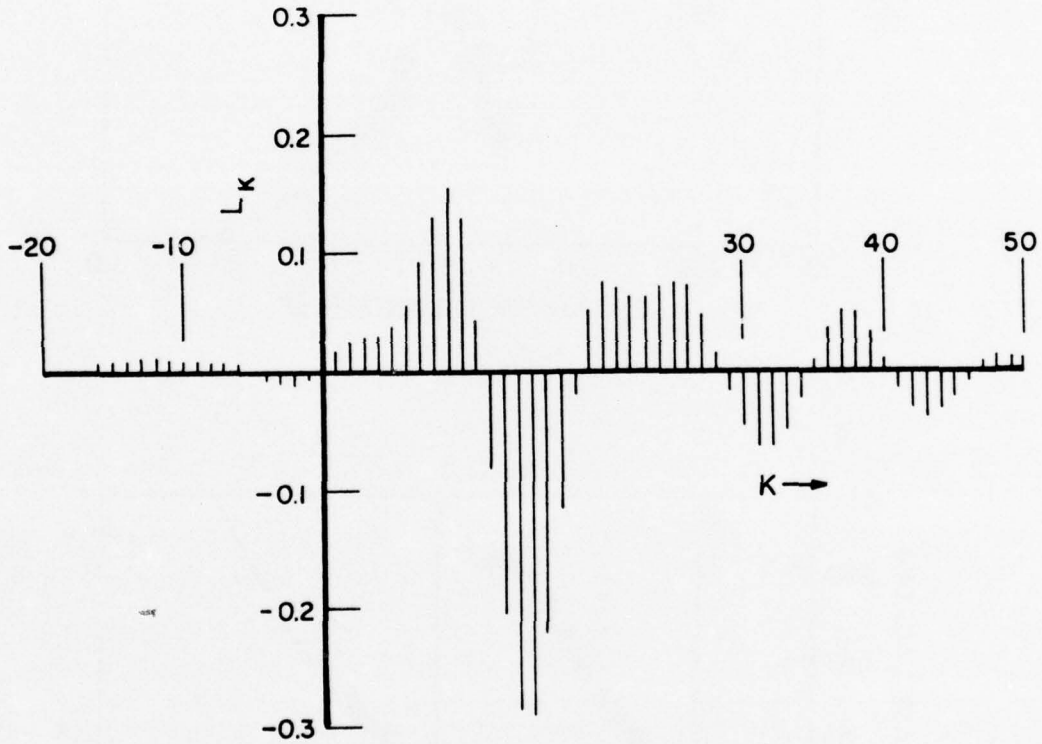

FIGURE 6 COEFFICIENTS, L_k, OF DISCRETE LINEAR IMPULSE RESPONSE CORRESPONDING TO FREQUENCY RESPONSE FUNCTION OF FIGURE 5

However, in the region of the bi-frequency plane of most practical interest (that is, near the mean added resistance operator) the experimental and analytical estimates are not impossibly different. Accordingly, the best choice for present purposes appeared to be the analytical result of Ref. 2.

The analytical quadratic frequency response function of Ref. 2 relates the quadratic part of added resistance to wave elevation at LCG. Thus the first necessary operation for the simulation was to develop the analytical quadratic frequency response function relating resistance to wave elevations one model length ahead of LCG. This was accomplished in accordance with the input filtering relationship, Eq. (26). Essentially, wave elevation ahead of model and at LCG are related in the wave frequency domain by the transfer function following Eq. (3). This transfer function becomes $L_1(\omega)$ after transformation into the encounter frequency domain.

Having thus made an initial estimate of the quadratic frequency response function, the process outlined in the discussion of Eq. (33) was pursued. The final results for the Q_{jk} weighting coefficients corresponding to the quadratic impulse response are shown in an isometric view in Figure 7. The weighting coefficient matrix is 71 x 71, and the value of the largest coefficient is 0.69. In the figure straight lines are drawn through the points along sections parallel to j and k axes so that each intersection corresponds to a value of Q_{jk}. Where the function is significant it is characterized by undulations in both j and k directions. Most of the negative values of the function are masked or indistinct, but are of roughly the same magnitude as the positive peaks shown. As may be noted at the edges of the plot, the truncation could have been at slightly higher values of j and k, but, as will be shown, the representation seems adequate. In this plot as in Figure 6 positive values of j and k correspond to the "past" of the wave elevation. The most significant part of the kernel lies in the region where both j and k are positive. There are weak interactions between positive k and negative j (and positive j and negative k by symmetry), but very little interaction response when both j and k are negative.

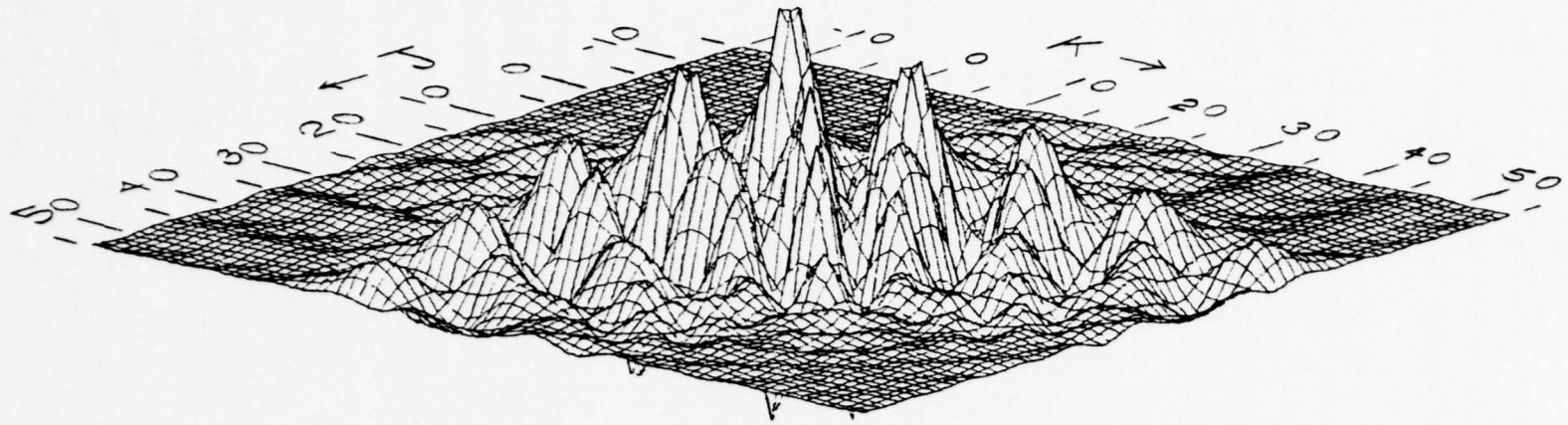

FIGURE 7 ISOMETRIC VIEW OF THE WEIGHTING COEFFICIENTS Q_{jk} RELATING THE QUADRATIC PART OF RESISTANCE TO WAVE ELEVATION ONE MODEL LENGTH AHEAD OF THE SERIES 60 MODEL AT FROUDE NUMBER 0.15

Agreement was quite good between the quadratic frequency response function corrected to wave forward of LCG and the re-transformation of the truncated, discrete function shown in Figure 7. The re-transformed function was then corrected to a wave phase reference at model LCG and is shown in comparison with the original analytical result of Ref. 2 in Figures 8 and 9. Figure 8 indicates the real part and Figure 9 the imaginary part of the function. These two figures are essentially plotted tables. The magnitude of the function involved is plotted in the non-dimensional bi-frequency plane (ω_1, ω_2). A second axis system is shown as well. This axis system is the "sum" and "difference" system defined by the transformations:

$$\Omega_1 = \omega_1 - \omega_2$$
$$\Omega_2 = \omega_1 + \omega_2 \qquad (34)$$

The Ω_1 and Ω_2 axes lie on the lines of symmetry.

The results from the re-transformation of the discrete kernel, Figure 7, are shown in the quadrant bounded by the $+\Omega_1$ and Ω_2 axes. In order to show the analytical results from Ref. 2 in the same figures, the octant bounded by the $+\omega_2$ and $+\Omega_2$ axes has been displaced in the negative Ω_1 direction. The analytical results are shown in this octant according to the basic symmetry properties of the quadratic frequency response function. If analytical results and the simulation were in exact agreement, the simulated results would be an exact reflection about the Ω_2 axis of the analytical results in the ω_2-Ω_2 octant. A similar procedure was adopted to show the analytical results corresponding to the simulated results in the ω_1-Ω_1 octant. In this case exact agreement would require that the simulated results would be an exact reflection about the Ω_1 axis of the analytical results in the Ω_1-$(-\omega_2)$ octant.

In order to emphasize the important parts of the function, estimates having absolute values less than 2.5 are omitted (blank). The contours shown are for the zero level.

BEST AVAILABLE COPY

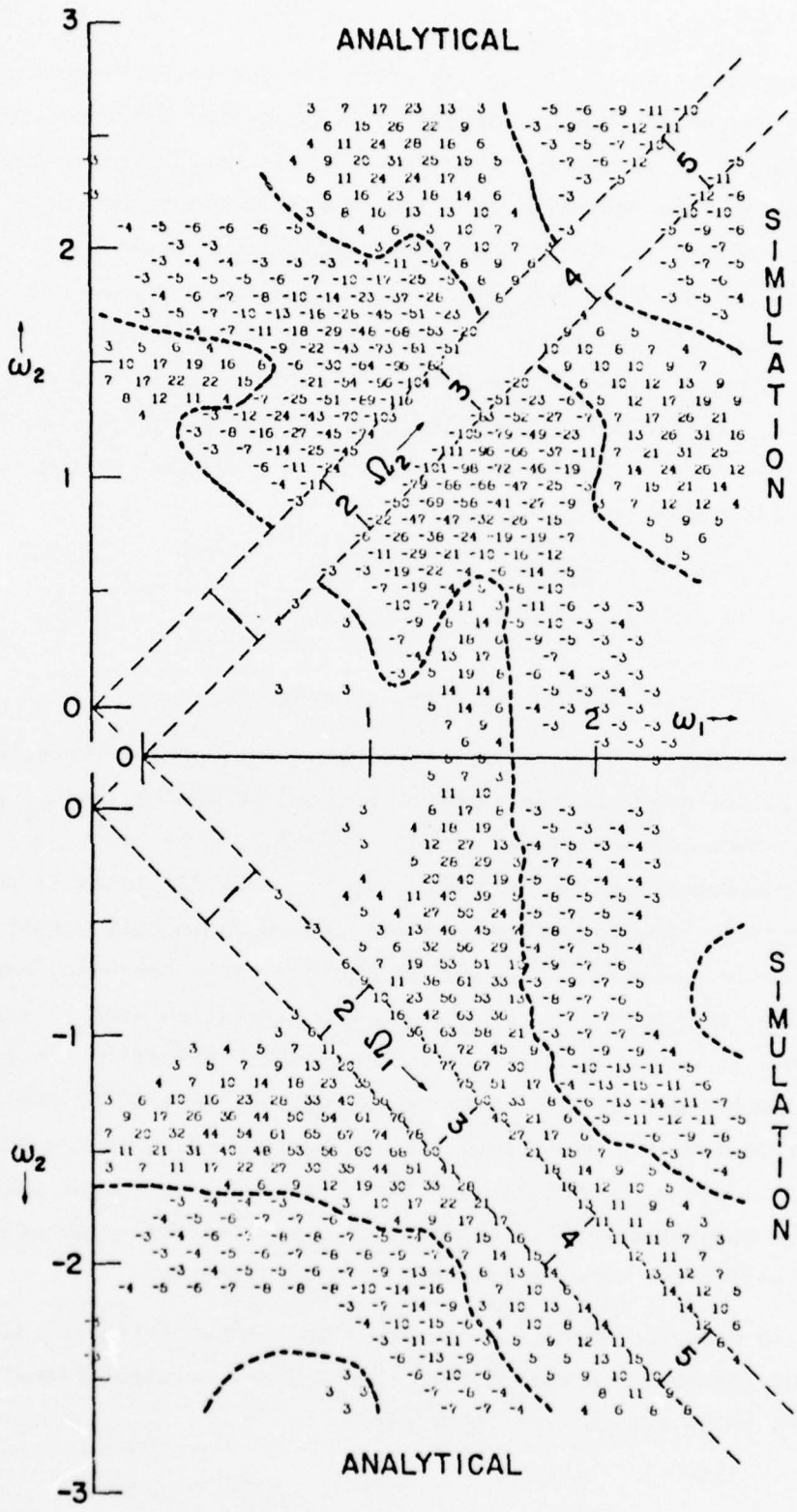

FIGURE 8 COMPARISON OF REAL PART OF ANALYTICAL AND SIMULATED QUADRATIC FREQUENCY RESPONSE FUNCTIONS FOR RESISTANCE WITH RESPECT TO WAVE AT LCG OF SERIES 60, 0.60 BLOCK MODEL AT FROUDE NUMBER 0.15

BEST AVAILABLE COPY

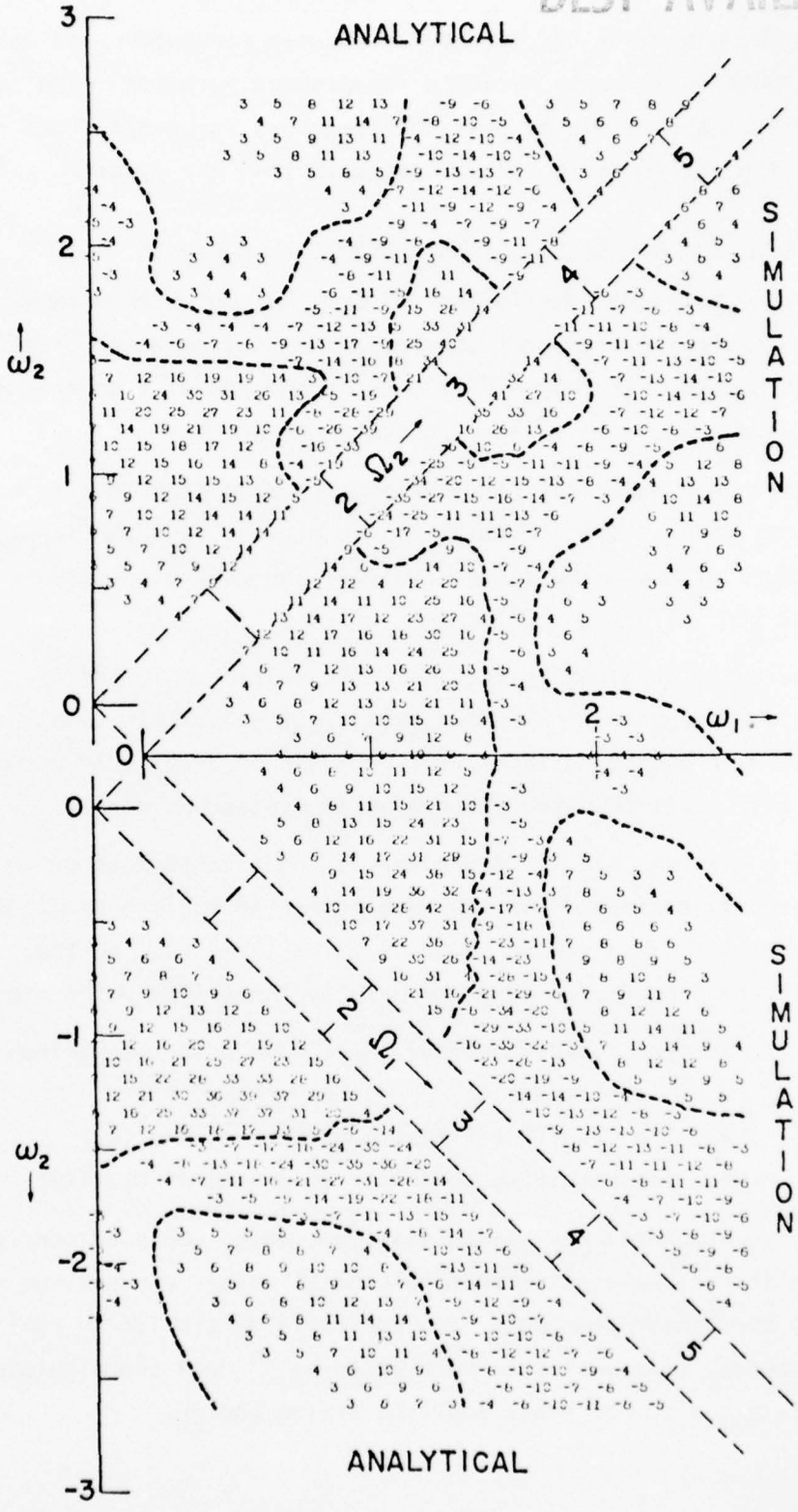

FIGURE 9 COMPARISON OF IMAGINARY PART OF ANALYTICAL AND SIMULATED QUADRATIC FREQUENCY RESPONSE FUNCTIONS FOR RESISTANCE WITH RESPECT TO WAVE AT LCG OF SERIES 60, 0.60 BLOCK MODEL AT FROUDE NUMBER 0.15

On the whole the correspondence between simulation and analytical result is considered quite adequate for present purposes. The re-transformation was carried out at half the frequency intervals shown in the figures. The intermediate values indicated that the function was smooth.

Computation of Sample Transient Responses

Having selected coefficients of Eq. (29) which were thought to fairly realistically represent the resistance characteristics of the assumed ship model, it remained only to do the convolution arithmetic for the example encountered wave pulses of Figure 4.

There is a numerical start-up and stopping transient in both convolutions in Eq. (29). However in the present case the input wave pulse is zero at beginning and end so that the resulting outputs do not have to be specially treated for this effect.

The basic programming used was that developed in Ref. 9. Before computing the response to the wave pulses the programming was run with sinusoidal wave elevation input, and analysis of results in accordance with Eq. (24) confirmed that the computing system was correct.

As a possible aid in interpretation, the components of Eq. (29) were separately evaluated for the wave pulses of maximum amplitude (Fig.4) and these results were stored separately for later use, so that the results of the computation were essentially three 1024 point time series:

1. The non-dimensional input wave pulse of maximum amplitude
2. The resulting linear component of Eq. (29)
3. The resulting quadratic component of Eq. (29)

To produce a simulated resistance transient which could be considered as the response to a wave pulse of amplitude (F) times the maximum shown in Figure 4, the linear component time series is multiplied by F, the quadratic component time series is multiplied by F^2, and the simulated transient is the sum of these modified series and g_o.

The basic results of the computation are shown in Figures 10 through 13. The wave pulses of Figure 4 were numbered; No. 1 corresponds to model arrival at mid-run 10 seconds early, No. 2 to arrival on time, and No. 3 to model arrival late. Figure 10 involves wave pulse No. 1, Figure 11 pulse No. 2 and Figure 12 pulse No. 3

In each of the figures the non-dimensionalized wave pulse is shown in the top frame, the linear and quadratic components of resistance in the next two frames, and finally at the bottom the simulated resistance (sum of the calm water resistance and the linear and quadratic components).

The time scale shown in the figures is essentially the point number of the time series. Only 300 points of the 1024 available were plotted for each case. The portions of the time series not shown are constant and equal to the values at beginning and end of the portions plotted. The vertical scales for each time history frame were chosen to best resolve the transient being plotted and are not the same from frame to frame.

Figure 13 illustrates the simulated results when the wave pulse is assumed to be less steep than maximum. In this case the simulated results for wave pulse No. 1 of maximum (full) amplitude are compared with the simulations for the cases when the wave pulse is assumed to involve wave elevations 1/2 and 1/4 the maximum shown in Figure 4.

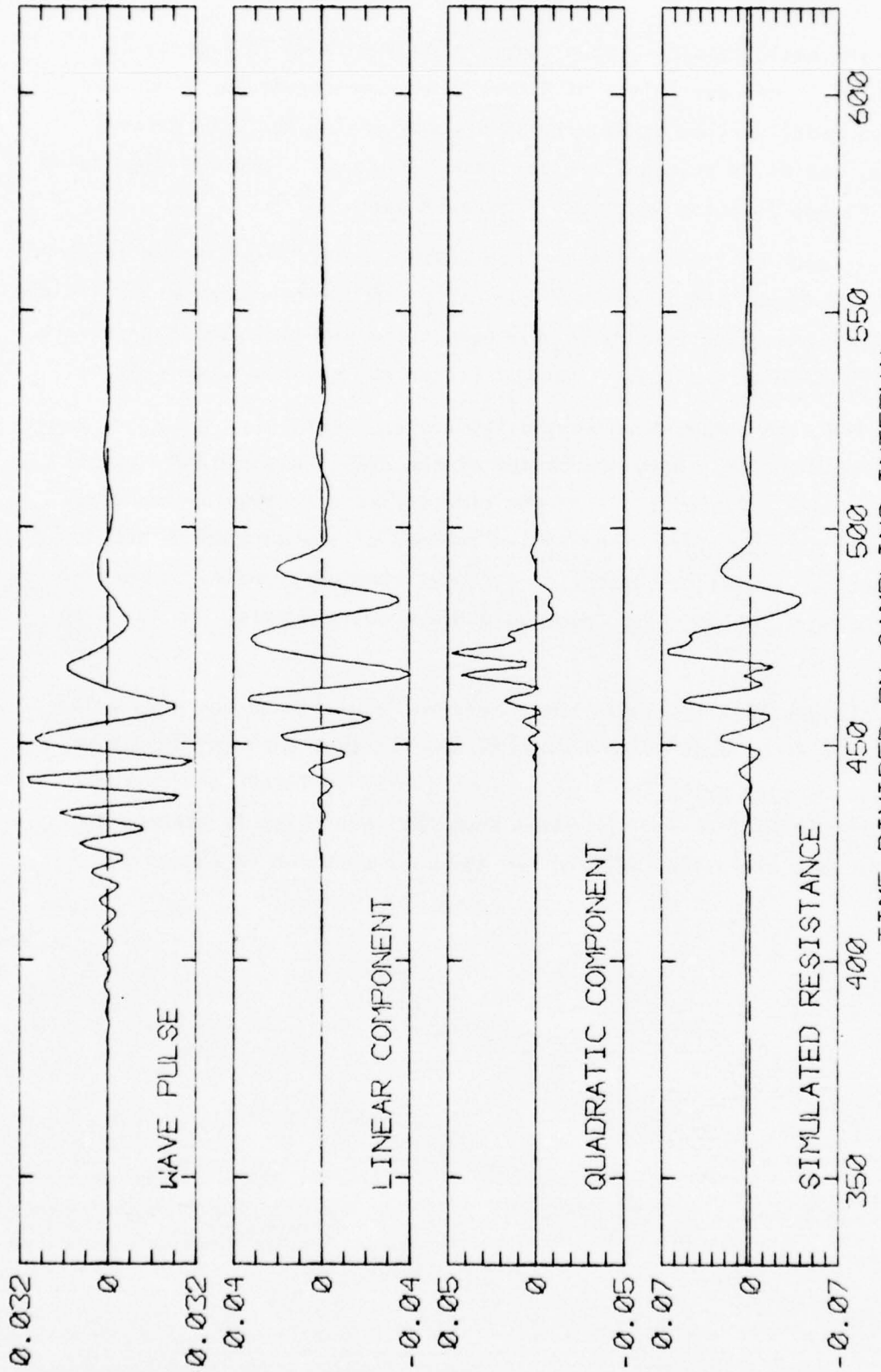

FIGURE 10 COMPONENTS AND SIMULATED RESISTANCE TRANSIENT RESPONSE TO WAVE PULSE NO. 1 OF MAXIMUM AMPLITUDE

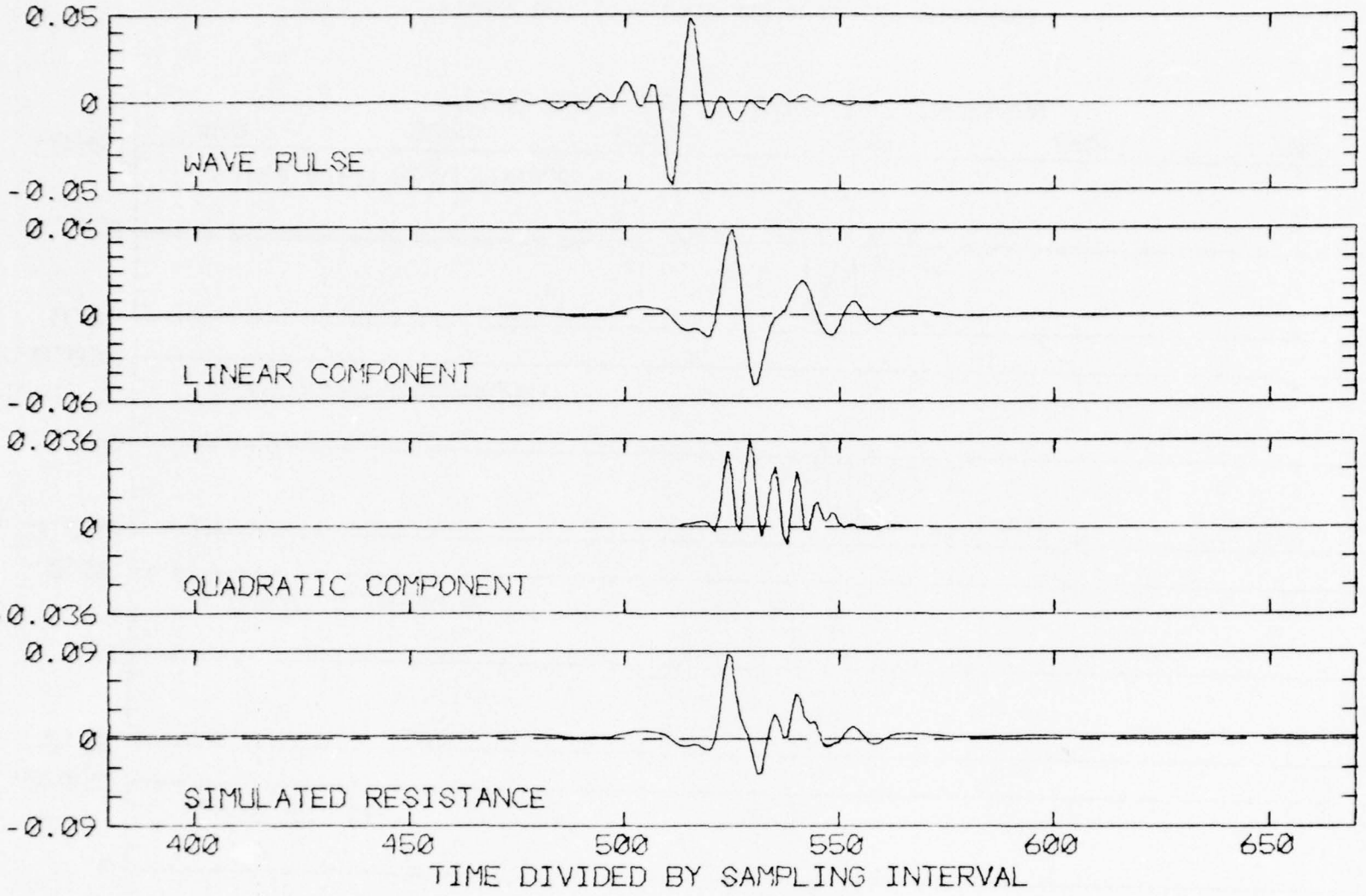

FIGURE 11 COMPONENTS AND SIMULATED RESISTANCE TRANSIENT RESPONSE TO WAVE PULSE NO. 2 OF MAXIMUM AMPLITUDE

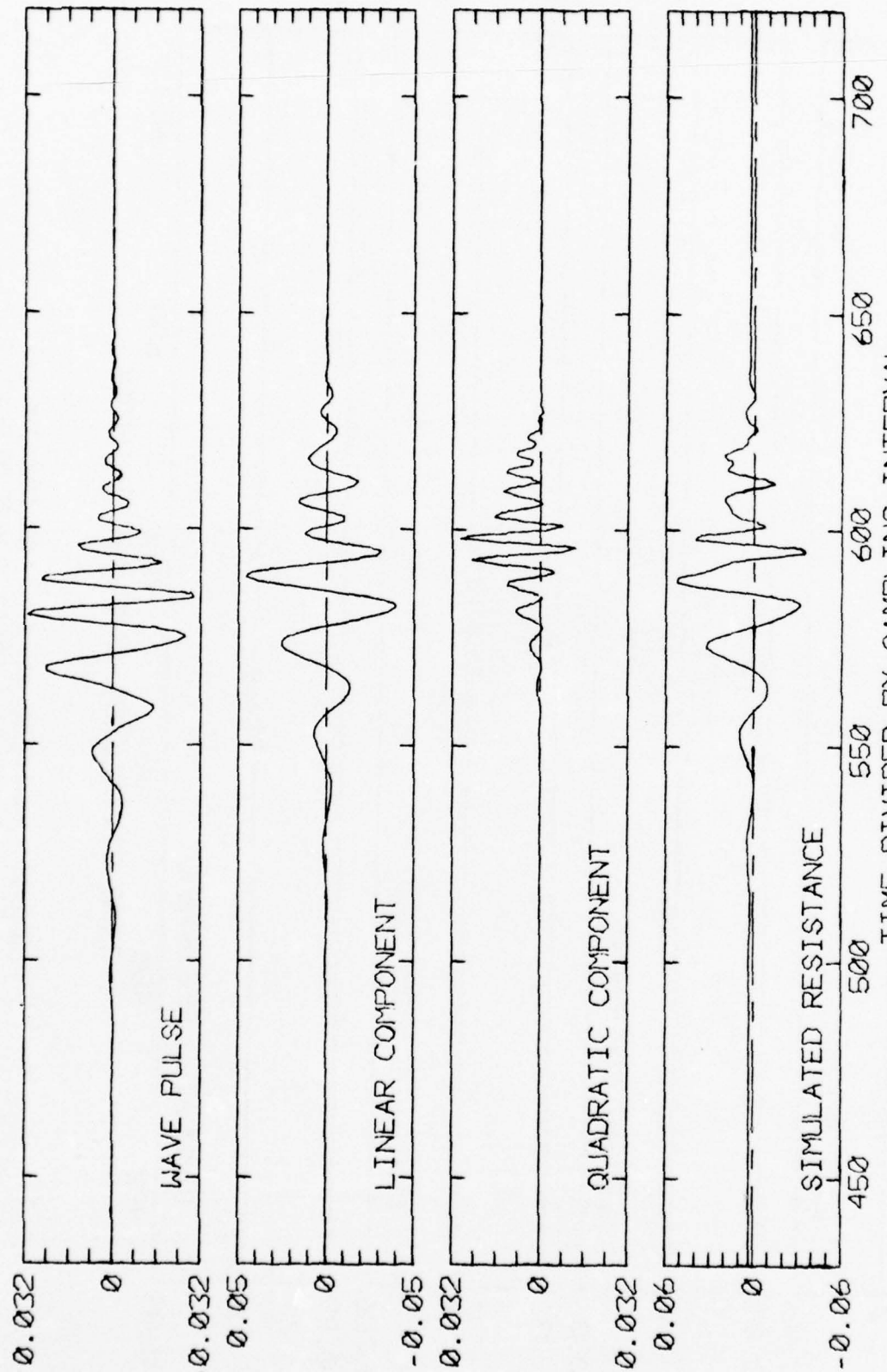

FIGURE 12 COMPONENTS AND SIMULATED RESISTANCE TRANSIENT RESPONSE TO WAVE PULSE NO. 3 OF MAXIMUM AMPLITUDE

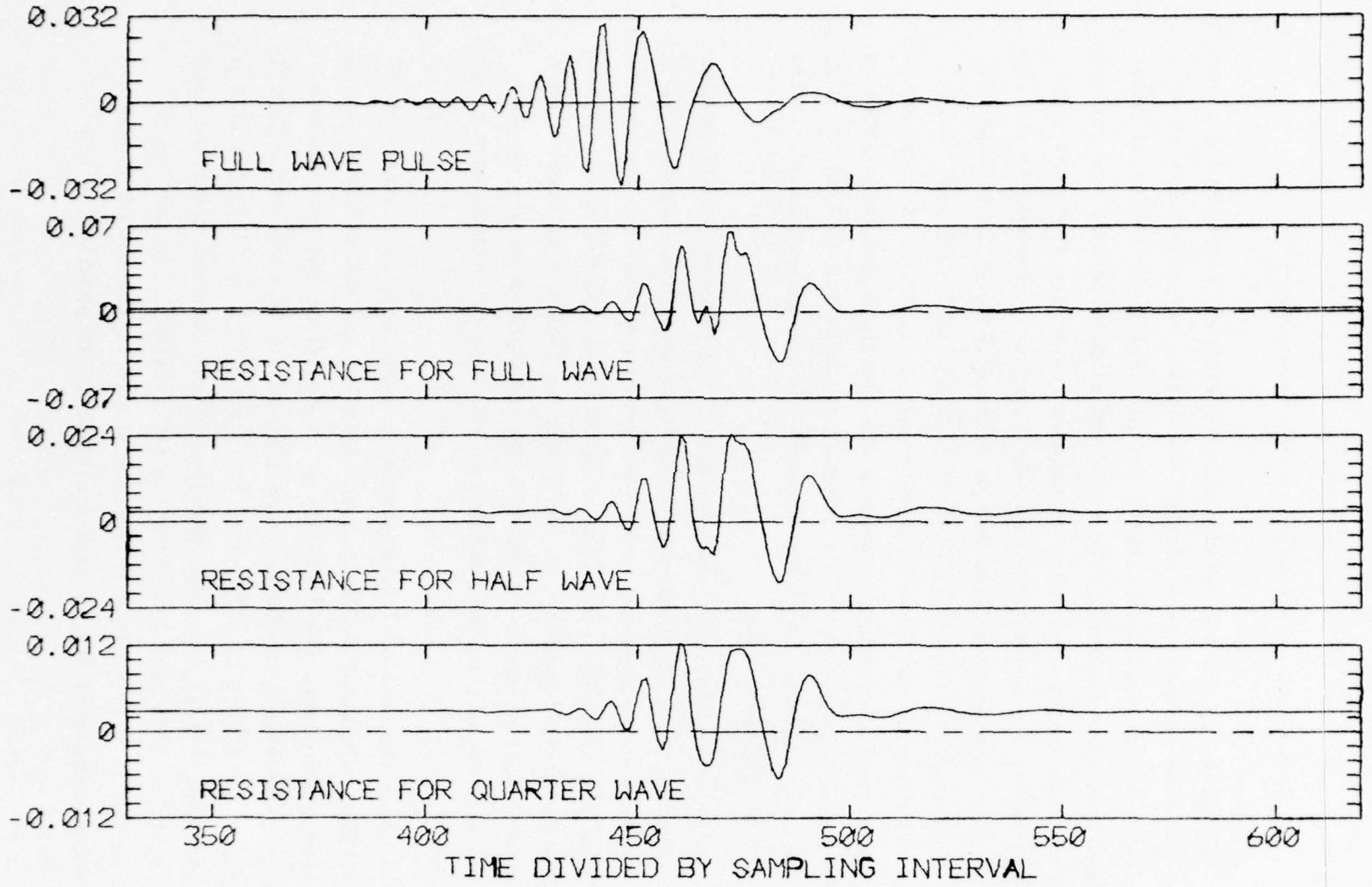

FIGURE 13 SIMULATED RESISTANCE TRANSIENT RESPONSE TO WAVE PULSE NO. 1 OF VARYING AMPLITUDE

DISCUSSION OF RESULTS OF RESISTANCE SIMULATION

In review of the simulated results presented in previous sections it may first be repeated that most of the detail was undertaken in an attempt to provide realistic results for one particular choice of model and experimental parameters. The experimental observations are conceptually confined to the wave pulse as observed by a wave probe one model length ahead of the model (top frames of Figures 10 through 13) and the resulting resistance transient (bottom frame of Figures 10 through 12). These simulated results are defined as time series in the same way as actual experimental data would be, after digitization. The components of resistance transients shown in Figures 10 through 12 are not observable. The frequency response functions shown in the previous section are also not available -- these (or parts thereof) are the answers sought in the analysis of the transients.

Within the particular assumptions of the hypothetical experiment (D.L. Tank No. 3, a five foot Series 60 model at Froude Number 0.15) the wave pulses developed appear to be realistic possibilities, and the total length of the simulated runs (including portions not plotted in Figures 10 through 13) is feasible. It would also be feasible to produce wave pulses of longer duration by altering the assumptions of a previous section with respect to the position in the tank of maximum wave concentration.

Given the feasibility of obtaining relatively long stretches of essentially calm water resistance at beginning and end of the observed resistance transient, the feasibility of the first and most obvious step in the anslysis of the resistance transient is confirmed. This is to remove the effect of calm water resistance (g_o) by fitting a straight line through initial and final portions of the observed transient, and then subtract this mean line from the observation. The portion of observation left after this correction should be the sum of linear and quadratic components due to wave excitation. In practice, since

electronic zero bias and possibly slight trends must be dealt with, this type of procedure would probably have to be carried out for the wave pulse as well so as to produce "zero" wave elevation at beginning and end of the observations.

The individual components of resistance shown in Figures 10 through 12 are about what would be expected from the input-output model. The linear component of resistance resembles a time lagged wave pulse insofar as symmetry about zero and apparent periods are concerned. The quadratic component does not much resemble the wave pulse except in duration. This component contains significant response at about half the apparent periods in the wave pulse and a visible relatively long period excursion of resistance so that the quadratic component of resistance is not symmetric about the mean.

The simulated total resistance transients in Figures 10 through 12 are visibly influenced by the quadratic component. These results are for a wave pulse of probable maximum intensity. It may be noted from Figure 13 that the appearance of the resistance transient is significantly influenced by the magnitude of the wave pulse. A comparison of the linear component of Figure 10 with the resistance for a wave pulse of 1/4 maximum amplitude in Figure 13 discloses that if the gain of the hypothetical wavemaker is reduced so that the wave steepnesses are 1/4 as great as the probable maximum obtainable, the obvious influence of the quadratic non-linearity on the total observed resistance transient all but disappears.

The foregoing is of course implicit in the input-output model assumed, and was observable in a sense in the irregular wave experiments described in References 6 and 9. In the examples herein the quadratic component of resistance is of the same magnitude as the linear part only for the wave pulses of an amplitude near the limit for propagation without substantial change in form. In practice, with recording equipment of more or less fixed dynamic range, it would be somewhat natural to opt for a relatively severe wave pulse when best resolution of the quadratic component is desired. On the other hand, the qualitative indications of Figure 13 suggest that isolation of the linear component might be achieved to acceptable accuracy if wave pulses of the mildest amplitude possible are employed.

INITIAL ANALYSIS OF QUADRATIC TRANSIENT RESPONSE

Existing Theoretical Methods

Among the most fundamental and useful engineering treatments of the functional input-output model (Barrett[10*], Bedrosian and Rice[11*], George[12*]) only George[12] treats the possibility of recovering the quadratic impulse or frequency response from transient experiments. The approach of the latter author involves successive isolation of the time domain kernels in a series of experiments. The first "experiment" is essentially the same as that implied in previous discussion and consists of observing that the system output for zero input is the zeroth degree kernel, g_o. The second series of "experiments" involves excitation of the system by ideal step functions of varying amplitudes. The resulting sets of output transients are expanded in a series in the amplitude of the step function for each of a number of successive values of time. The coefficients of the first power of the step amplitude form a function of time and the linear impulse response is its derivative with respect to time. The third series of "experiments" involves excitation of the system with two step functions which are separated by a known time delay, τ. This is repeated for a series of step amplitudes as before, and a series expansion in step amplitude is made. After utilizing some results of the second experiment, the coefficients of the second power of the step amplitude form a function of time, t, and time delay, τ. The whole procedure must be repeated for different values of τ so that finally a two-dimensional function of time (say τ_1 and τ_2) is generated. The quadratic impulse response is effectively the partial derivative with respect to τ_1 and τ_2.

---

*10. Barrett, J.F., "The Use of Functionals in the Analysis of Non-Linear Physical Systems," Journal of Electronics and Control, Vol. 15, No. 6, December 1963.

*11. Bedrosian, E. and Rice, S.O., "The Output Properties of Volterra Systems (Nonlinear Systems with Memory) Driven by Harmonic and Gaussian Inputs," Proceedings of the IEEE, Vol. 59, No. 12, December 1971.

*12. George, D.A., "Continuous Non-Linear Systems," Doctoral Dissertation, Department of Electrical Engineering, M.I.T., July 1959.

The above procedure depends critically upon the properties of ideal step functions, and, accordingly, this procedure is unworkable for the present problem. It is not possible to generate wave steps, ideal or otherwise. In fact, judging by the numerical results shown in Figure 4, it is doubtful that it would be feasible to so control the various experimental parameters that wave pulses of exactly the same shape but different amplitudes could be encountered by the model. Even if wave steps were physically possible, the multiple run requirement would make the approach unattractive since the only point in developing a transient test technique is to make one test run do the work of many.

Correlation and Fourier Integral Analysis

First intuition suggested that analysis of the non-linear transient might be approached in grossly the same manner as the previous analyses of the random process with quadratic non-linearity[1]. Clearly, most of the techniques available for analysis of linear random systems have their counterpart in the analysis of linear transients. The most important difference is that the operation of taking the statistical expectation in the random analysis is replaced in the transient analysis by integration over all time. The expectation or mean value of the type of wave induced transients shown herein clearly tends to zero as the limits of integration are increased without bound.

In the analyses to follow the n-dimensional form of Parseval's Theorem (Barrett[10]) was used extensively, and, for reference, it is reproduced as follows:

$$\int\int\cdots\int f_1(t_1,t_2\cdots t_n)\,f_2(t_1,t_2,\cdots t_n)\,dt_1\,dt_2\cdots dt_n$$

$$= \frac{1}{(2\pi)^n}\int\int\cdots\int F_1^*(\omega_1,\omega_2\cdots\omega_n)\,F_2(\omega_1,\omega_2,\cdots\omega_n)\,d\omega_1\,d\omega_2\cdots d\omega_n \qquad (35)$$

where the (*) denotes complex conjugate and $f_j(t_1\cdots)$ and $F_j(t_1\cdots)$ are Fourier Transform pairs defined:

$$F_j(\omega_1,\omega_2\cdots\omega_n) = \iint\cdots\int f_j(t_1,t_2\cdots t_n)\,\mathrm{Exp}(-i\sum_{r=1}^{n}\omega_r t_r)\,dt_1\,dt_2\cdots dt_n$$

$$f_j(t_1,t_2\cdots t_n) = \frac{1}{(2\pi)^n}\iint\cdots\int F_j(\omega_1,\omega_2\cdots\omega_n)\,\mathrm{Exp}(i\sum_{r=1}^{n}\omega_r t_r)\,d\omega_1\cdots d\omega_n \qquad (36)$$

The simplest operation on the resistance transient is integration over time. Using the basic model, Eq. (18), and transposing the constant, g_o:

$$\int(r(t)-g_o)\,dt = \iint g_1(t_1)h(t-t_1)\,dt\,dt_1 + \iint g_2(t_1,t_2)\int h(t-t_1)h(t-t_2)\,dt\,dt_1\,dt_2 \qquad (37)$$

Noting that the first term on the right hand side is zero for a zero-mean wave pulse, and applying the Parseval Theorem:

$$\int(r(t)-g_o)\,dt = \frac{1}{2\pi}\int G_2(\omega,-\omega)\,|\,H(\omega)\,|^2\,d\omega \qquad (38)$$

where $H(\omega)$ is the Fourier Transform of the wave pulse. The integral of the wave induced part of $r(t)$ is non-zero in general and in form is the same as the expression for the expected value of resistance in random seas[1], the squared absolute value of the complex wave pulse spectrum being analogous to the scalar spectrum of the random waves. The operation yields no approach to the identification of the mean added resistance operator, $G_2(\omega,-\omega)$.

The next integral operation which is common in analysis of the linear case is a lagged product. Forming the lagged product of resistance transient and wave pulse, and substituting Eq. (18):

$$\begin{aligned} m_1(\tau) &= \int r(t)h(t-\tau)\,dt \\ &= g_o\int h(t-\tau)\,dt \\ &+ \iint g_1(t_1)h(t-t_1)h(t-\tau)\,dt_1\,dt \\ &+ \iiint g_2(t_1,t_2)h(t-t_1)h(t-t_2)h(t-\tau)\,dt_1\,dt_2\,dt \end{aligned} \qquad (39)$$

The first observation about Eq. (39) is that the integral multiplied by

g_o is zero within the zero mean wave pulse assumption. Utilizing the Parseval Theorem to modify the succeeding integrals there results:

$$M_1(\omega) = \frac{1}{2\pi}\int m_1(\tau)\,\mathrm{Exp}[-i\omega\tau]d\tau$$

$$= G_1(\omega)\,|\,H(\omega)\,|^2$$

$$+ \frac{1}{4\pi}H^*(\omega)\int G_2\left(\frac{\omega+\beta}{2},\frac{\omega-\beta}{2}\right)H\left(\frac{\omega+\beta}{2}\right)H\left(\frac{\omega-\beta}{2}\right)d\beta \qquad (40)$$

where inside the second integral the frequency parameters ω and β correspond to the sum and difference frequencies, Ω_2 and Ω_1 which are defined by Eqs. (34). If the system had been entirely linear the integral would be zero and the result would be exactly as expected for linear systems. In the case of random wave excitation the analogous integral dropped out because the excitation was assumed to be zero-mean Gaussian, and the expected value of triple products of Gaussian variables is zero. Thus while simple cross-correlation analysis is fruitful in identification of the linear term from random data, it does not appear useful in the case of transient data since only the elimination of the constant term is effected.

Proceeding with the analogy with the analysis of random data, a double lagged product may be defined:

$$m_2(\tau_1,\tau_2) = \int h(t+\tau_1)h(t-\tau_1)[r(t-\tau_2)-g_o]dt$$

$$= \iint g_1(t_1)h(t-\tau_2-t_1)h(t+\tau_1)h(t-\tau_1)dt_1\,dt$$

$$+ \iiint g_2(t_1,t_2)h(t-\tau_2-t_1)h(t-\tau_2-t_2)h(t+\tau_1)h(t-\tau_1)dt_1\,dt_2\,dt \qquad (41)$$

This product is essentially the same as the product used in the derivation of the cross-bi-spectrum. The difference is in the integration with time instead of the expected value operator.

Applying the Parseval Theorem to the integrals of Eq. (41) there results:

$$M_2(\tau_1,\omega) = \int m_2(\tau_1,\tau_2)\,\mathrm{Exp}[-i\omega\tau_2]\,d\tau_2$$

$$= H_2(\omega,\tau_1)\left\{G_1^*(\omega)H^*(\omega) + \frac{1}{4\pi}\int G_2^*\left(\frac{\omega+\beta}{2},\frac{\omega-\beta}{2}\right)H^*\left(\frac{\omega+\beta}{2}\right)H^*\left(\frac{\omega-\beta}{2}\right)d\beta\right\} \quad (42)$$

where

$$H_2(\omega,\tau) = \int h(t-\tau)\,h(t+\tau)\,\mathrm{Exp}[-it\omega]\,dt \quad (43)$$

and ω and β of the second integral are the same as those in Eq. (40). The terms within curly brackets differ from Eq. (40) virtually only by a factor of $H(\omega)$. The quadratic frequency response function is imbedded in an integral. No separation of linear and quadratic frequency response functions has been effected for exactly the same reasons as in the previous case for the single lagged product. The formation of the lagged product as a function of τ_1 is seen to be redundant. If τ_1 is considered constant and equal to zero in Eq. (41), the function of τ_2 which results corresponds to the lagged product of resistance and the squared wave pulse. The result of this variation is exactly the same in form as Eq. (42).

A final integral analysis of interest is the Fourier Transform of the resistance transient, $R(\omega)$. The resistance transient and its Fourier transform are a transform pair as follows:

$$R(\omega) = \int r(t)\,\mathrm{Exp}[-i\omega t]\,dt \quad (44)$$

$$r(t) = \frac{1}{2\pi}\int R(\omega)\,\mathrm{Exp}[i\omega t]\,d\omega \quad (45)$$

Manipulating the integrals in the basic input-output model, Eq. (18), by means of the Parseval Theorem, the Fourier transform of the resistance transient becomes:

$$R(\omega) = 2\pi g_o\,\delta(\omega) + G_1(\omega)H(\omega) + \frac{1}{4\pi}\int G_2\left(\frac{\omega+\beta}{2},\frac{\omega-\beta}{2}\right)H\left(\frac{\omega+\beta}{2}\right)H\left(\frac{\omega-\beta}{2}\right)d\beta \quad (46)$$

where $\delta(\omega)$ is the Dirac delta function. This is the expression analogous

to the scalar spectrum of resistance in the random excitation case[1], and the form is very similar. Since H(0) must be zero for a zero mean wave pulse, R(0) may be seen to be the integral of the wave induced resistance, Eq. (38), plus a delta function arising from the constant calm water resistance.

Reviewing the results in Eqs. (40), (42) and (46) it is clear that the correlation and Fourier Integral approaches do not immediately suggest any general methods for data reduction. No separation of linear and quadratic terms is evident. The quadratic frequency response function appears in an integral, and this integral is practically the same regardless of the initial approach. Simple Fourier Transformation of the resistance transient and wave pulse results in information of exactly the same nature as that found by correlation techniques.

Some explanation of the result is afforded by supposing that the quadratic impulse response is known, as well as an input transient h(t). Under these circumstances a function of two times, t and τ, may be developed:

$$p(t,\tau) = \iint g_2(t_1,t_2)\,h(t-t_1)\,h(\tau-t_2)\,dt_1\,dt_2 \tag{47}$$

Applying the Parseval Theorem to Eq. (47):

$$\begin{aligned} P(\omega_1,\omega_2) &= \iint p(t,\tau)\,\mathrm{Exp}[-i\omega_1 t - i\omega_2 \tau]\,dt\,d\tau \\ &= G_2(\omega_1,\omega_2)\,H(\omega_1)\,H(\omega_2) \end{aligned} \tag{48}$$

Given the function $p(t,\tau)$ and the input transient h(t) Eq. (48) implies a simple identification method for $G_2(\omega_1,\omega_2)$. However, it may be seen by comparing Eq. (47) with the quadratic term of Eq. (18) that the quadratic component of resistance is the value of the function $p(t,\tau)$ when $\tau=t$. Effectively, the time variable τ is lost and is not directly recoverable when only the transient quadratic resistance component is known. In none of the correlation approaches attempted was it possible to achieve the equivalent of the situation in Eq. (47) where the arguments in the two input transients do not have a common term.

What was sought in attempting correlation methods was some means of developing from the observables a function of time or time lags which is a double Fourier transform of the quadratic frequency response function. Failure to find such a function in the present work does not prove that it is impossible to do so. However the nature of the quadratic model is such that it seems possible that insufficient information is contained in a single resistance transient to enable a more or less direct identification of the complete quadratic frequency response function.

A FILTERING APPROACH TO SEPARATION OF LINEAR AND QUADRATIC COMPONENTS

The unsolved problems of the last section may be considered in two parts: 1) The quadratic component of the resistance was not isolated and, 2) the quadratic frequency response function appears in an integral. Of these two problems, the first is at least as critical as the second since the linear component of the transient would be expected to be dominant in most experimental cases. Even if the integral can be inverted in some way, the linear component amounts to a "noise" which is large relative to the quadratic signal.

The prospects for something useful resulting from a filtering operation on the resistance transient are best discussed in conjunction with the Fourier Transform, Eq. (46). Figure 14 shows the computed moduli of the Fourier Transforms of the various components of the simulated results for wave pulse No. 1 (Figure 10). At the top is the modulus of the wave pulse transform, $|H(\omega)|$. In the middle the modulus of the linear component, $|G_1(\omega)H(\omega)|$, is shown as a solid line. Superposed in dashes is the modulus of the transform of the quadratic component (the integral in Eq.46). Finally the modulus of the transform of the total resistance, $|R(\omega)|$, is shown at the bottom.

It is clear from the example in Figure 14, as well as the form of the integral in Eq. (46), that the quadratic component of resistance has some frequency components the same as those produced by the linear part of the system. If all the linear components are eliminated by some sort of filtering a great deal of whatever information is contained in the quadratic component will also be eliminated.

To be more specific, suppose the resistance transient corresponding to Figure 14 is passed through a low-pass filter with cutoff frequency adjusted so that all frequency components above a non-dimensional frequency of 0.5 are attenuated to much less than 1% of their original magnitude. Under these circumstances practically all of the linear contribution to

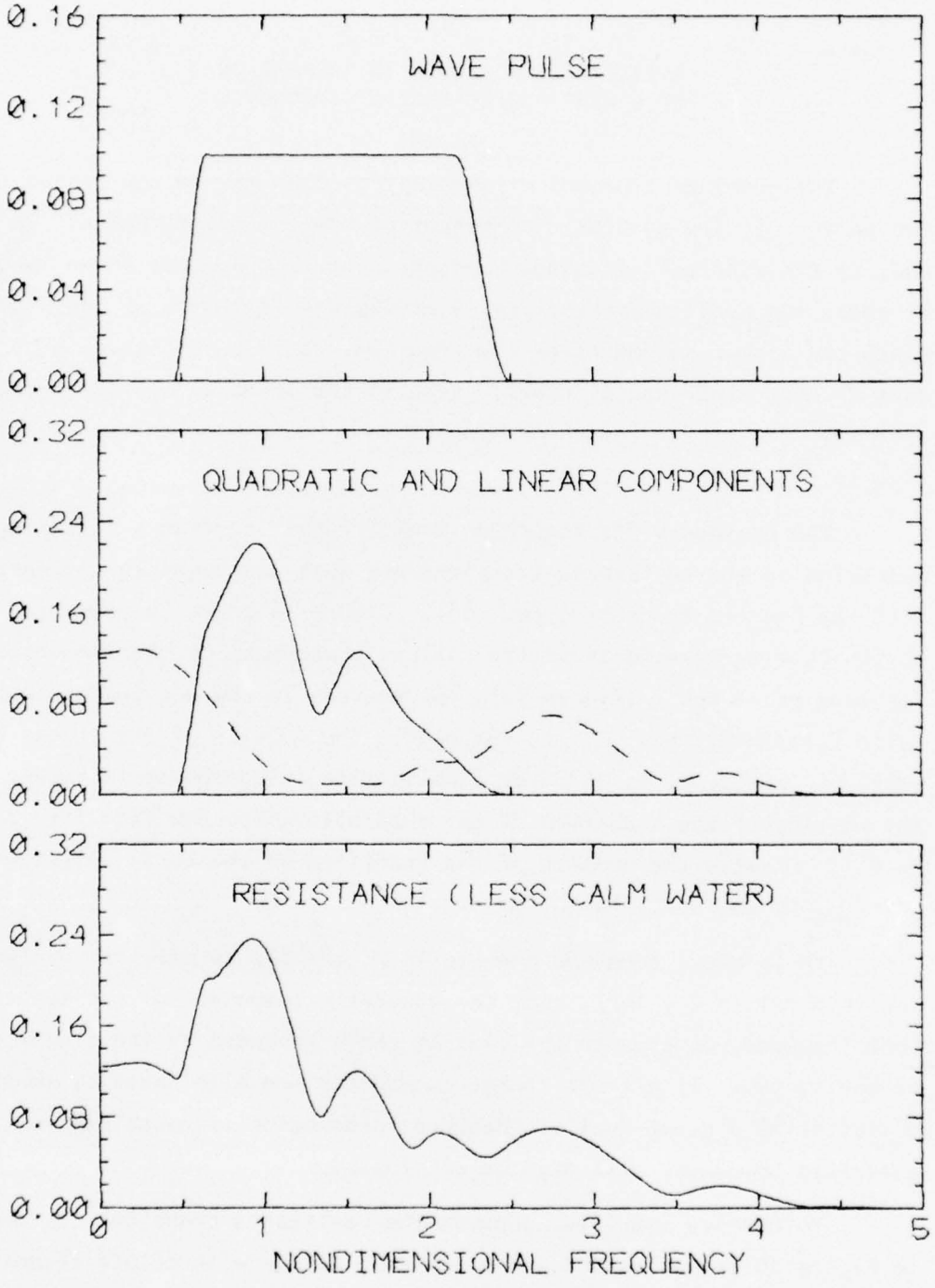

FIGURE 14 MODULII OF COMPUTED FOURIER TRANSFORMS OF SIMULATED RESISTANCE COMPONENTS, WAVE PULSE NO. 1

the transform, Figure 14, disappears, as well as the quadratic contribution to the transform above a frequency of 0.5. What is left of the resistance transform will be at frequencies below the lowest wave pulse frequency, and what will be left in the time domain will be only a relatively long period excursion of resistance. In terms of the quadratic frequency response function what is thrown away by this operation is defined by the filtering equation, Eq. (28). Referring to Figures 8 and 9 the low-pass filtering operation just described produces an apparent quadratic frequency response function which is zero or negligible for $|\Omega_2|$ greater than 0.5, and which is appreciable only near the position of the mean added resistance operator (the Ω_1 axis, Figs.8,9). So long as the low-pass filter has unity DC gain, the apparent quadratic frequency response function after filtering contains the mean added resistance operator undistorted.

Thus a straightforward low-pass filtering operation appeared to have some promise if estimates of the quadratic frequency response function in the neighborhood of the mean added resistance operator are all that is desired. Because the mean added resistance operator is the only part of the quadratic response function which has found practical application, the approach appeared worthwhile pursuing.

To formalize the low pass filtering approach somewhat, it is first required that a low-pass filter frequency response function, $L_e(\omega)$, be specified so that

$$G_1(\omega)H(\omega)L_e(\omega)$$

is zero or approaches zero for all frequencies. The filter should have unity DC gain. Because the linear component of resistance can have appreciable frequency components only at frequencies at which the wave pulse has appreciable frequency components, the specification of the cutoff frequency of the filter may be made on the basis of the frequency of the lowest appreciable frequency component of the wave pulse. Knowing this frequency, the filter cutoff must be adjusted so as to attenuate resistance components at this frequency to some very small fraction of the original.

Supposing the filter to be selected in this way, an expression for the filtered resistance, $r_1(t)$, may be written with the aid of Eqs. (28), (45) and (46):

$$r_1(t) \approx g_o L_e(0) + \frac{1}{8\pi^2} \iint G_2\left(\frac{\omega+\beta}{2}, \frac{\omega-\beta}{2}\right) L_e(\omega) H\left(\frac{\omega+\beta}{2}\right) H\left(\frac{\omega-\beta}{2}\right) \mathrm{Exp}[i\omega t] d\beta d\omega \qquad (49)$$

where as in previous equations, ω corresponds to the sum or output frequency and β to the difference frequency.

The elimination of the calm water resistance, g_o, from Eq. (49) may be made as has been previously suggested. This is to fit a straight line through beginning and end of the filtered transient and subtract the result from the transient itself. Then after filtering and correction for the calm water resistance what is left may be called $r_2(t)$ and is written:

$$r_2(t) \approx \frac{1}{8\pi^2} \iint G_2\left(\frac{\omega+\beta}{2}, \frac{\omega-\beta}{2}\right) L_e(\omega) H\left(\frac{\omega+\beta}{2}\right) H\left(\frac{\omega-\beta}{2}\right) \mathrm{Exp}[i\omega t] d\beta d\omega \qquad (50)$$

In Eq. (50) $L_e(\omega)$ is specified by the filter, $H(\omega)$ is the Fourier Transform of the encountered wave pulse, and $r_2(t)$ is the result of filtering the observed resistance transient and correcting this result for calm water resistance. Only the quadratic frequency response function, $G_2(\omega_1, \omega_2)$ is considered unknown.

Temporarily leaving aside the question of whether anything can be done with Eq. (50), some practical filtering considerations may be dealt with. The foremost question is whether the specified filter can be realized. In the hypothetical experiment the wave pulse is supposed to be under sufficient control so that the influence of frequency components below some lowest encounter frequency is nil. The lowest encounter frequency is determined by the longest wave length assumed to be important and by model speed. In the present example if the longest wave length of importance is fixed as shown in Figure 2 and the Froude number is varied, the lowest wave encounter frequency of importance varies only by ± 10% from that shown in Figure 14 for model speeds ranging from zero to twice

that of the example. Accordingly the filtering situation as defined by Figure 14 may be taken as typical. In this case in order to substantially eliminate frequency components above a non-dimensional frequency of 0.5, something like a six pole filter with nominal cutoff frequency of 0.25 is required.

If the basic data is digitized before filtering, two methods are available with which filters of the above specification may be realized. The easiest is perhaps the FFT based fast convolution. In the present example a recursive digital filter is difficult because of the very low cutoff in relation to the folding frequency range (in the example the Δt chosen results in a folding frequency 30 times the required filter cutoff). However it is feasible to implement a two stage digital filtering procedure where the first stage removes enough high frequency response so that the data may be decimated, and the second stage, operating on the decimated data, achieves the desired final filter cutoff.

Alternately, there is the possibility of incorporating a real analog filter into the experimental instrumentation. The non-dimensional encounter frequencies noted in Figure 14 are almost numerically equal to real frequencies (in Herz) for the 5 foot model size described. Six-pole low-pass filters with fixed cutoff frequency of 0.25 Hz are not now off-the-shelf items, but solid-state electronic modules with which such a cutoff may be realized are readily available. In situations where the model is "large", say 20 feet, the filter cutoff would have to be in the neighborhood of 0.1 Hz. These cutoff frequencies are also considered within reason for modern equipment and the alternative of incorporating real filters into the experiment is also assumed to be feasible. In such a case the data digitized for analysis would be the filtered output.

Ideally there would be no preference between digital and analog filtering -- only a matter of whether high frequency content would be thrown away at the outset or after the experiment is over. In practice, preference might be given to analog filtering during the experiment. Judging by the examples previously shown, the filtered resistance excursion is apt to be small relative to the maximum peak to peak range of

the total resistance transient. Real time analog filtering would make possible the adjustment of gains so that the best use is made of the resolution available on the recording medium -- a particularly important consideration if the recording medium is analog magnetic tape.

AN APPROXIMATE APPROACH TO THE IDENTIFICATION OF THE MEAN ADDED RESISTANCE OPERATOR

Presuming that the linear component of the resistance transient may be removed one way or another by filtering there is left Eq. (50), which has the form of a pure quadratic system. The function to be identified is $G_2(\frac{\beta}{2}, -\frac{\beta}{2})$. Continuing the approach in the last section, if the pass band of the filter $L_e(\omega)$ is reduced even further than is required to eliminate the linear component, the effective quadratic frequency response function is concentrated along the line $\omega_1=-\omega_2$ ($\Omega_2=0$, Figures 8,9).

Considering the variation of the actual quadratic frequency response function near the line $\omega_1=-\omega_2$, according to the general symmetry properties of the function it is expected that

$$\frac{\partial}{\partial\omega} G_2\left(\frac{\omega+\beta}{2},\frac{\omega-\beta}{2}\right)\Bigg|_{\omega=0} \rightarrow [0 + iF_1(\beta)]$$

in which $F_1(\beta)$ is an even function in β. Accordingly, for values of ω not far from zero it would be expected that the quadratic frequency response function would have the form:

$$F_R(\beta) + i\omega F_1(\beta)$$

in which $F_R(\beta)$ is the mean added resistance operator $[G_2(\frac{\beta}{2}, -\frac{\beta}{2})]$, and is even in β.

Now if it is assumed that the low pass filter can be made sufficiently narrow, the effective quadratic frequency response function may be approximated by:

$$K_2\left(\frac{\omega+\beta}{2},\frac{\omega-\beta}{2}\right) \cong L_a(\omega)[F_R(\beta) + i\omega F_I(\beta)] \tag{51}$$

In the approximation it is assumed that $L_a(0)=1$ so that $F_R(\beta)$, the function of interest, is not distorted. It is further assumed that $L_a(\omega)$ is nearly zero for values of ω for which $[F_R(\beta)+i\omega F_I(\beta)]$ is not a good representation of the actual frequency response function.

The filter in the above approximation is assumed to be an analysis filter which has a lower cutoff frequency than any real filter which might have been applied before digitizing the data. There is no reason why this filter has to be realizable in the real time sense, and some convenience in taking it as non-realizable. Thus $L_a(\omega)$ will be taken as real and even in ω.

In general, the approximation, Eq. (51) must correspond to an effective quadratic impulse response, $k_2(t_1,t_2)$. Applying Eq. (20):

$$k_2(t_1,t_2) = \frac{1}{(2\pi)^2}\iint \mathrm{Exp}[i\omega_1 t_1 + i\omega_2 t_2]K_2(\omega_1,\omega_2)\,d\omega_1\,d\omega_2$$

$$= \frac{1}{2}\frac{1}{(2\pi)^2}\iint \mathrm{Exp}\left[i\omega\frac{t_1+t_2}{2} + i\beta\frac{t_1-t_2}{2}\right]K_2\left(\frac{\omega+\beta}{2},\frac{\omega-\beta}{2}\right)d\omega d\beta \tag{52}$$

(after making the usual transformation; $\omega=\omega_1+\omega_2$, and $\beta=\omega_1-\omega_2$)

Letting:
$$T_2 = \frac{t_1+t_2}{2}$$
$$T_1 = \frac{t_1-t_2}{2} \tag{53}$$

and substititing Eq. (51) into Eq. (52), and noting that $F_R(\beta)$ and $F_I(\beta)$ are even in β, and that $L_a(\omega)$ is even in ω, there is finally obtained:

$$k_2(t_1,t_2) = \frac{1}{2}\ell_a(T_2)\cdot f_1(T_1) + \frac{1}{2}\ell_b(T_2)\cdot f_2(T_1) \tag{54}$$

where:

$$\ell_a(T_2) = \frac{1}{2\pi} \int L_a(\omega) \cos T_2 \omega d\omega \tag{55}$$

$$\ell_b(T_2) = \frac{-1}{2\pi} \int \omega L_a(\omega) \sin T_2 \omega d\omega \tag{56}$$

$$f_1(T_1) = \frac{1}{2\pi} \int F_R(\beta) \cos T_1 \beta d\beta \tag{57}$$

$$f_2(T_1) = \frac{1}{2\pi} \int F_I(\beta) \cos T_1 \beta d\beta \tag{58}$$

The apparent quadratic impulse response Eq. (54) has the correct symmetry. Interchange of t_1 and t_2 leaves T_2 unchanged, and T_1 negative, but the function is the same because both Eq. (57) and (58) are even in T_1. Equations (55) and (56) are just Fourier sine and cosine transforms of a filter frequency response which is specified. Given what is known about the quadratic frequency response function the left hand sides of Eq. (57) and (58) are expected to be absolutely integrable so that the inverses may be written:

$$F_R(\beta) = \int f_1(T_1) \text{Exp}[-i\beta T_1] dT_1$$

$$= \int f_1(T_1) \cos T_1 \beta dT_1 \tag{59}$$

(since $f_1(T_1)$ is even in T_1)

similarly:

$$F_I(\beta) = \int f_2(T_1) \cos T_1 \beta dT_1 \tag{60}$$

Now assuming that the analysis filter has been applied to the resistance transient and the calm water resistance has been corrected for, the result (denoted $r_3(t)$) may be written:

$$r_3(t) = \iint k_2(t_1, t_2) h(t-t_1) h(t-t_2) dt_1 dt_2 \tag{61}$$

Equation (61) is exactly analogous to the third term of Eq. (18). Application of the Parseval Theorem would result in a form exactly the same as Eq. (50) with the substitution of Eq. (51) for the effective quadratic frequency response function.

Substituting Eq. (54) in Eq. (61) and making the variable transformation defined by Eq. (53) there results:

$$r_3(t) \cong \int f_1(T_1) \int \ell_a(T_2) h(t-T_2-T_1) h(t-T_2+T_1)\, dT_2\, dT_1$$

$$+ \int f_2(T_1) \int \ell_b(T_2) h(t-T_2-T_1) h(t-T_2+T_1)\, dT_2\, dT_1 \qquad (62)$$

Alternately, by replacing the quadratic frequency response in the third term of Eq. (46) by the approximation, Eq. (51) there results the Fourier transform of $r_3(t)$:

$$R_3(\omega) \cong \frac{1}{4\pi} \int L_a(\omega) [F_R(\beta) + i\omega F_I(\beta)] H\left(\frac{\omega+\beta}{2}\right) H\left(\frac{\omega-\beta}{2}\right) d\beta \qquad (63)$$

In either form the result of the approximation to the apparent quadratic frequency response is to separate an unknown function of two variables into the product of a known function and an unknown function of one variable. Equations (62) and (63) are equivalent in the sense that application of the Parseval Theorem, Eq. (35), to Eq. (62) yields Eq. (63).

A start at a practical data reduction method based upon Eq. (62) or (63) was first made by considering Eq. (62), the time domain version. Because the simulated transients correspond to response to a wave elevation forward of the model it is known from the work of Refs. 1 and 6 that the imaginary part of the function near the mean added resistance operator will vary strongly, that is, $F_I(\beta)$ will be relatively large. However, it was shown in Refs. 1 and 6 that a simple time shift of input relative to output tends to minimize the magnitude of the imaginary part of the function near the line $\omega_1 = -\omega_2$. In the case of the present simulation the actual best time shift is the same as that in Ref. 6, or 18 points. In order to simplify a first trial it seemed reasonable to assume that the shifting operation would make $F_I(\beta)$ very small (that is, the imaginary part of the effective quadratic frequency response function would be nil). Under this further approximation $f_2(T_1)$, (Eq.58) is also negligible and the filtered, time shifted resistance response was approximated as:

$$r_4(t) \approx \int f_1(T_1) \int \ell_a(T_2) h(t-T_2-T_1) h(t-T_2+T_1)\, dT_2\, dT_1 \qquad (64)$$

For purposes of an actual digital computation it was assumed that the same type of representation which had produced the simulated transients (Eq.29) would be adequate. Thus to transpose to the digital form:

$$t = p\Delta t$$
$$T_1 = j\Delta t$$
$$T_2 = k\Delta t$$

and Eq. (64) becomes:

$$r_4(p) = \sum_j \sum_k f_{1j} \ell_{ak} h(p-k-j) h(p-k+j) \tag{65}$$

where $h(p-k-j)$ and $h(p-k+j)$ represent points on the time history at time steps $(p-k-j)$ and $(p-k+j)$. Similarly, $r_4(p)$ is the resistance time history at time step p. In Eq. (65) discrete approximations to $f_1(T_1)$ and $\ell_a(T_2)$ were made as follows:

$$f_1(T_1) = f_{1j}\, \delta(T_1 - j\Delta t) \tag{66}$$

$$\ell_a(T_2) = \ell_{aj}\, \delta(T_2 - k\Delta t) \tag{67}$$

Now taking the Fourier transforms of Eq. (66) and (67); there results:

$$\bar{F}_R(\beta) = f_{10} + 2 \sum_j f_{1j} \cos(j\beta\Delta t) \qquad j=1,2\ldots \tag{68}$$

$$\bar{L}_a(\omega) = \ell_{ao} + 2 \sum_k \ell_{ak} \cos(k\omega\Delta t) \qquad k=1,2\ldots \tag{69}$$

Manipulating Eq. (65) slightly,

$$r_4(p) = \sum_j f_{1j}\, C_{pj} \qquad j=0,1,2\ldots \tag{70}$$

where

$$C_{pj} = q_j \sum_{k=-m}^{m} \ell_{ak} h(p-k-j) h(p-k+j) \tag{71}$$

with $q_o = 1$

$q_j = 2$ for $j \neq 0$

Once the filter impulse response (ℓ_{ak}) is specified, Eq. (71) is calculable as a function of j for each response time step, p. Accordingly, Eq. (70) represents a series of linear algebraic equations in the unknown discrete impulse response, f_{1j}. It was hoped that this series of equations could be solved in a least squares sense for the f_{1j}, and thus ultimately estimates could be made of $F_R(\beta)$ via Eq. (68).

The steps done in trying this approach out were as follows:

a. Compensate the simulated resistance transient for calm water resistance.

b. Assume a Hanning Type Filter and compute ℓ_{ak}:

$$\ell_{ak} = \frac{1}{E}[1+\cos\pi k/m] \tag{72}$$

where:

$$E = \sum_{k=-m}^{m} [1+\cos\pi k/m]$$

and m is chosen to control the cutoff. Specifically, the corresponding frequency response, $\bar{L}_a(\omega)$ is unity for $\omega=0$ and roughly 1/2 for $\omega=\pi/m\Delta t$.

c. Compute $\bar{L}_a(\omega)$, Eq. (69).

d. Filter the resistance transient with $\bar{L}_a(\omega)$ utilizing the FFT fast convolution method.

e. Shift the wave pulse time series relative to the resistance time series as previously noted.

f. Compute C_{pj} for each point in the wave time series, and accumulate the coefficients in a least squares fit of Eq. (70).

g. Scale the coefficients in the resulting L.S. fit equations as required.

h. Solve for the f_{1j} using a standard Gauss elimination technique (Subroutine GELG or DGELG, IBM Scientific Subroutine Package).

i. Estimate $\bar{F}_R(\beta)$ via Eq. (68) using the results of step h.

The above procedure was applied to the simulated sets of transient data with various choices of m, that is, various choices of low pass filter cutoff. The number of estimates of f_{1j} solved for was varied from 10 to 30. In no case were the results of the procedure meaningful. Double precision accumulation of L.S. fit coefficients and solution for f_{1j} was necessary in order to get any sort of solution for the case that the scaling (step g) involved only division of the entire set of equations by the largest absolute value in the coefficient matrix. A scaling procedure was devised with which all the coefficients on the left hand coefficient matrix were of the order of unity and by which each row and column of the coefficient matrix contain a value near unity. The solution after this scaling was no more meaningful than those mentioned previously.

The coefficient matrix obtained in step f of the procedure is certainly numerically ill-conditioned. Those answers which were returned for the f_{1j} were typically alternately positive and negative and of about the same magnitude irrespective of the magnitude of j. To see what answer should have been obtained, the simulated added resistance operator, Figure 8, was transformed numerically in accordance with Eq. (57) and evaluated at a time step corresponding to that used in the analysis. These results indicated that the absolute values of the f_{1j} should have decreased as j increased, the magnitude should have been small enough to disregard after 30 time steps, and that semi-oscillations plus to minus should have been about 4 time steps. This evidence along with the nature of the fitted results suggested an over-fit. Thus ill-conditioning appears not to be merely numerical but that there is really not enough independent information left after the heavy filtering operation to enable a solution for the 30 or so values of f_{1j} which seem to be required for a reasonable estimate of the mean added resistance operator.

There is of course the possibility that the assumption that $F_1(\beta)$ is negligible is at fault. However, the low pass filtering operation plus the shifting, was certainly enough to make the imaginary part of

the apparent quadratic frequency response function relatively small, if not negligible. Given that the results obtained under the assumption of negligible $F_1(\beta)$ were not even in the ballpark it was doubted that a procedure involving Eq. (62) rather than Eq. (64) would be worth the substantially increased effort, and accordingly the above approach was abandoned.

Some effort was made to develop a similar procedure with Eq. (63), the frequency domain version of Eq. (62). Referring to Eq. (63), the product:

$$L_a(\omega)H(\tfrac{\omega+\beta}{2})H(\tfrac{\omega-\beta}{2})$$

is calculable from the Fourier transforms of the wave pulse. In addition to a relative time shift, a re-location of the (arbitrary) position of time = 0 was advisable before carrying out the Fourier transform on both the wave and resistance transients so that the arguments of each were slowly varying. The net result of the development was an estimation equation of the form:

$$\begin{aligned} R_3(\omega) = &\int F_R(\beta)\ C_1(\omega,\beta) \\ &+ \int F_I(\beta)\ C_2(\omega,\beta) \\ &+ i \int F_R(\beta)\ C_3(\omega,\beta) \\ &+ i \int F_I(\beta)\ C_4(\omega,\beta) \end{aligned} \tag{73}$$

in which the $C_n(\omega,\beta)$ are calculable functions of ω and β. This approach was carried through in a similar manner to that indicated in Eq. (65) through (71). The results obtained after applying the approach were just as bad as before -- regardless of whether $F_1(\beta)$ was assumed to be negligible or not. The basic problem with this approach is that after applying the Fast Fourier Transform to the resistance transient and carrying out the low-pass filtering there are a limited number of values of $R_3(\omega)$ available. In the present case with 1K arrays defining the transient, and a filter narrow enough to eliminate the linear component of resistance, there were only a dozen or so estimates of $R_3(\omega)$ which were not

negligible due to the effect of the low-pass filter. Thus $F_R(\beta)$ and $F_I(\beta)$ needed to be approximated by no more than a dozen discrete values along the β axis from zero the the folding frequency. This frequency resolution is much too coarse for a practical data reduction procedure. On paper, the solution would be to add zeros to the transient arrays, doubling their length so that more estimates could be obtained in the pass-band of the filter. This approach is thought illusory and was not attempted because all that is achieved is an interpolation -- no new and independent information is achieved. Just as in the time domain approach, the few results achieved with the frequency domain approach indicated that there is really not enough independent information left after filtering to allow reasonable answers.

CONCLUDING REMARKS

Because the experimental determination of the characteristics of mean ship model resistance added by waves is one of the more difficult and time consuming problems in seakeeping towing tank practice, it was of practical interest to see if a technique involving wave pulses could be developed, and if so, if it promised better efficiency.

Toward this end a fairly realistic digital simulation was made of the head wave pulse experiment and of the resulting resistance transient. There appears to be little doubt that such an experiment is feasible, and that the influence of calm water resistance can be eliminated in a straightforward way because the "memory" of the nonlinear part of the added resistance is not exorbitantly long.

The development of a data reduction procedure was approached from the point of view that any practically attractive data reduction procedure must involve a very few wave pulse runs, preferably only one. This point of view was re-inforced by the wave pulse simulation because it appeared that the detailed shape of the wave pulse would be seriously affected by small changes in wavemaker and model control parameters. For example, wave pulse time histories of exactly the same shape but different amplitudes appear to require more precise control of experiment than is ordinarily possible. Accordingly it appeared that if reasonable estimates could not be obtained from one experiment, there would be little point in attempting methods which required multiple experiments for any purpose other than confirmation,or for improving quality of estimates through simple averaging.

Several correlation and Fourier analysis approaches to the identification from transient data of the quadratic frequency response function for added resistance were investigated. All the approaches were analogous to one or another of the known approaches for outputs of linear and quadratic systems in response to random excitation. None of these investigations

resulted in a clean approach to the problem. Evidence was developed that a conceptually clean approach may be impossible. With respect to a recovery of the entire quadratic frequency response function for added resistance, it appears that insufficient information is contained in a single transient. It should be remarked that this is in contrast to the case for random Gaussian excitation. In this latter case a clean approach arises and is traceable to statistical properties of the expected values of products of input.

By taking advantage of the general properties of the quadratic model which appears to be valid for added resistance, it was possible to develop a "dirty" approach for the identification of the mean added resistance operator from a single transient experiment. However no meaningful results could be obtained with this latter approach. Those results which were obtained imply that there is not enough information in a single transient experiment to enable the identification of even a special portion of the quadratic frequency response function (the mean added resistance operator).

It appears that if there is a practical wave pulse technique for added resistance experiments, it is not yet in hand.

REFERENCES

1. Dalzell, J.F., "Application of the Functional Polynomial Model to the Ship Added Resistance Problem," Eleventh Symposium on Naval Hydrodynamics, London, March 1976.

2. Dalzell, J.F. and Kim, C.H., "Analytical Investigation of the Quadratic Frequency Response for Added Resistance," SIT-DL-76-1878, Davidson Laboratory, Stevens Institute of Technology, August 1976.

3. Davis, M.C. and Zarnick, E.E., "Testing Ship Models in Transient Waves," Fifth Symposium on Naval Hydrodynamics, Bergen, 1964.

4. Takezawa, S. and Takekawa, M., "Advanced Experimental Techniques for Testing Ship Models in Transient Water Waves: Part I, The Transient Test Technique on Ship Motions in Waves," Eleventh Symposium on Naval Hydrodynamics, London, 1976.

5. Takezawa, S. and Hirayama, T., "Advanced Experimental Techniques for Testing Ship models in Transient Water Waves: Part II, The Controlled Transient Water Waves for Using in Ship Motion Tests," Eleventh Symposium on Naval Hydrodynamics, London, 1976.

6. Dalzell, J.F., "Application of Cross-Bi-Spectral Analysis to Ship Resistance in Waves," SIT-DL-72-1606, AD 749102, Davidson Laboratory, Stevens Institute of Technology, May 1972.

7. Sibul, O.J., "Constant Thrust vs. Constant Velocity Method for Resistance Measurement in Waves," University of Calibornia, Berkeley, Report NA-71-1, June 1971.

8. Journee, J.M.J., "Motions, Resistance and Propulsion of a Ship in Longitudinal Regular Waves," Report 428, Laboratorium voor Sheepshydromechanica, Technische Hogeschool Delft, May 1976.

9. Dalzell, J.F., "The Applicability of the Functional Polynomial Input-Output Model to Ship Resistance in Waves," SIT-DL-75-1794, Davidson Laboratory, Stevens Institute of Technology, January 1975.

10. Barrett, J.F., "The Use of Functionals in the Analysis of Non-Linear Physical Systems," Journal of Electronics and Control, Vol. 15, No. 6, December 1963.

11. Bedrosian, E. and Rice, S.O., "The Output Properties of Volterra Systems (Nonlinear Systems with Memory) Driven by Harmonic and Gaussian Inputs," Proceedings of the IEEE, Vol. 59, No. 12, December 1971.

12. George, D.A., "Continuous Non-Linear Systems," Doctoral Dissertation, Department of Electrical Engineering, M.I.T., July 1959.

PRINCIPAL NOTATION

$F_R(\beta)$, $F_I(\beta)$	approximating functions
$f_1(T_1)$, $f_2(T_1)$	impulse responses
f_{1j}	weighting coefficients
$G_1(\omega)$	linear frequency response function
$G_2(\omega_1, \omega_2)$	quadratic frequency response function
g	gravitational constant
g_o	zeroth degree kernel (calm water resistance)
$g_1(t)$	linear kernel (surge force impulsive response)
$g_2(t_1, t_2)$	quadratic kernel (added resistance impulse response)
$H(\omega)$	Fourier transform of wave pulse
$h(t)$	encountered wave pulse
$h_x(t)$	wave pulse at tank position x
j,k,p	indices
$L_1(\omega)$, $L_2(\omega)$ $L_a(\omega)$, $L_e(\omega)$	linear frequency responses (filters)
L_j	linear weighting coefficient
$\ell_a(T_2)$, $\ell_b(T_2)$	impulse responses
Q_{jk}	quadratic weighting coefficients
$r(t)$	resistance transient

T_1, T_2	time variables
t	time
U	model velocity
X, X_m	tank position
β	difference frequency
Δt	time interval
τ_1, τ_2, τ	dummy time variables
Ω_1	difference frequency
Ω_2	sum frequency (equals encounter frequency)
ω, ω_1, ω_2	encounter frequency
$\underline{\omega}$	wave frequency
ω_{1L}	frequency of wave of ship length

DISTRIBUTION LIST
Contract N00014-76-C-0348

40 Commander
David W. Taylor Naval Ship
Research and Development Center
Bethesda, MD 20084
Attn: Code 1505 (1)
Code 5211.4 (39)

1 Officer-in-Charge
Annapolis Laboratory
Naval Ship Research and
Development Center
Annapolis, MD 21402
Attn: Code 522.3 (Library)

7 Commander
Naval Sea Systems Command
Washington, DC 20362
Attn: SEA 09G32 (3 cys)
SEA 03512 (Peirce)
SEA 037
SEA 0322
SEA 033

12 Director
Defense Documentation Center
5010 Duke Street
Alexandria, VA 22314

1 Office of Naval Research
800 N. Quincy Street
Arlington, VA 22217
Attn: Mr. R.D. Cooper (Code 438)

1 Office of Naval Research
Branch Office
492 Summer Street
Boston, MA 02210

1 Office of Naval Research
Branch Office (493)
536 S. Clark Street
Chicago, IL 60605

1 Chief Scientist
Office of Naval Research
Branch Office
1030 E. Green Street
Pasadena, CA 91106

1 Office of Naval Research
Resident Representative
715 Broadway (5th Floor)
New York, NY 10003

1 Office of Naval Research
San Francisco Area Office
760 Market St., Rm 447
San Francisco, CA 94102

2 Director
Naval Research Laboratory
Washington, DC 20390
Attn: Code 2027
Code 2629 (ONRL)

1 Commander
Naval Facilities Engineering
Command (Code 032C)
Washington, DC 20390

1 Library of Congress
Science & Technology Division
Washington, DC 20540

8 Commander
Naval Ship Engineering Center
Department of the Navy
Washington, DC 20362
Attn: SEC 6034B
SEC 6110
SEC 6114H
SEC 6120
SEC 6136
SEC 6144G
SEC 6140B
SEC 6148

1 Naval Ship Engineering Center
Norfolk Division
Small Craft Engr. Dept.
Norfolk, VA 23511
Attn: D. Blount (6660.03)

1 Library (Code 1640)
Naval Oceanographic Office
Washington, DC 20390

1 Commander (ADL)
Naval Air Development Center
Warminster, PA 18974

1 Naval Underwater Weapons Research
& Engineering Station (Library)
Newport, RI 02840

1 Commanding Officer (L31)
Naval Civil Engineering Laboratory
Port Hueneme, CA 93043

3 Commander
Naval Ocean Systems Center
San Diego, CA 92132
Attn: Dr. A. Fabula (6005)
Dr. J. Hoyt (2501)
Library (13111)

1 Library
Naval Underwater Systems Center
Newport, RI 02840

1 Research Center Library
Waterways Experiment Station
Corps of Engineers
P.O. Box 631
Vicksburg, MS 39180

1 Dept. of Transportation
Library TAD-491.1
400 - 7th Street S.W.
Washington, DC 20590

1 Charleston Naval Shipyard
Technical Library
Naval Base
Charleston, SC 29408

1 Norfolk Naval Shipyard
Technical Library
Portsmouth, VA 23709

1 Philadelphia Naval Shipyard
Philadelphia, PA 19112
Attn: Code 240

1 Portsmouth Naval Shipyard
Technical Library
Portsmouth, NH 03801

1 Puget Sound Naval Shipyard
Engineering Library
Bremerton, WA 98314

1 Long Beach Naval Shipyard
Technical Library (246L)
Long Beach, CA 90801

1 Hunters Point Naval Shipyard
Technical Library (Code 202.3)
San Francisco, CA 94135

1 Pearl Harbor Naval Shipyard
Code 202.32
Box 400, FPO
San Francisco, CA 96610

1 Mare Island Naval Shipyard
Shipyard Technical Library
Code 202.3
Vallejo, CA 94592

1 Assistant Chief Design Engineer
for Naval Architecture (Code 250)
Mare Island Naval Shipyard
Vallejo, CA 94592

2 U.S. Naval Academy
Annapolis, MD 21402
Attn: Technical Library
Dr. Bruce Johnson

1 Naval Postgraduate School
Monterey, CA 93940
Attn: Library, Code 2124

1 Study Center
National Maritime Research Center
U.S. Merchant Marine Academy
Kings Point, L.I., NY 11204

1 U.S. Merchant Marine Academy
Kings Point, L.I., NY 11204
Attn: Academy Library

1 Bolt, Beranek & Newman
50 Moulton Street
Cambridge, MA 02138
Attn: Library

1 Bethlehem Steel Corporation
Center Technical Division
Sparrows Point Yard
Sparrows Point, MD 21219

1 Bethlehem Steel Corporation
25 Broadway
New York, NY 10004
Attn: Library (Shipbuilding)

1 Esso International
Design Division, Tanker Dept.
15 West 51st Street
New York, NY 10019

1 Mr. V. Boatwright, Jr.
R & D Manager
Electric Boat Division
General Dynamics Corporation
Groton, CT 06340

1 Gibbs & Cox, Inc.
21 West Street
New York, NY 10006
Attn: Technical Info. Control

1 Hydronautics, Inc.
Pindell School Road
Howard County
Laurel, MD 20810
Attn: Library

1 McDonnell Douglas Aircraft Co.
3855 Lakewood Blvd.
Long Beach, CA 90801
Attn: T. Cebeci

1 Lockheed Missiles & Space Co.
P.O. Box 504
Sunnyvale, CA 94088
Attn: Mr. R.L. Waid, Dept 57-74
Bldg. 150, Facility 1

1 Newport News Shipbuilding &
Dry Dock Company
4101 Washington Avenue
Newport News, VA 23607
Attn: Technical Library Dept.

1 Nielsen Engineering & Research Inc.
510 Clude Avenue
Mountain View, CA 94043
Attn: Mr. S. Spangler

1 Oceanics, Inc.
Technical Industrial Park
Plainview, L.I., NY 11803

1 Society of Naval Architects
and Marine Engineers
74 Trinity Place
New York, NY 10006
Attn: Technical Library

1 Sun Shipbuilding & Dry Dock Co.
Chester, PA 19000
Attn: Chief Naval Architect

1 Sperry Systems Management Division
Sperry Rand Corporation
Great Neck, NY 11020
Attn: Technical Library

1 Stanford Research Institute
Menlo Park, CA 94025
Attn: Library G-021

2 Southwest Research Institute
P.O. Drawer 28510
San Antonio, TX 78284
Attn: Applied Mechanics Review
Dr. H. Abramson

1 Tracor, Inc.
6500 Tracor Lane
Austin, TX 78721

1 Mr. Robert Taggart
3930 Walnut Street
Fairfax, VA 22030

1 Ocean Engr. Department
Woods Hole Oceanographic Inst.
Woods Hole, MA 02543

1 Worcester Polytechnic Inst.
Alden Research Laboratories
Worcester, MA 01609
Attn: Technical Library

1 Applied Physics Laboratory
University of Washington
1013 N.E. 40th Street
Seattle, WA 98105
Attn: Technical Library

1 University of Bridgeport
Bridgeport, CT 06602
Attn: Dr. E. Uram

4 University of California
Naval Architecture Department
College of Engineering
Berkeley, CA 94720
Attn: Library
Prof. W. Webster
Prof. J. Paulling
Prof. J. Wehausen

3 California Institute of Technology
Pasadena, CA 91109
Attn: Aeronautics Library
Dr. T.Y. Wu
Dr. A.J. Acosta

1 Docs/Repts/Trans Section
Scripps Institution of
Oceanography Library
University of California, San Diego
P.O. Box 2367
La Jolla, CA 92037

1 Catholic University of America
Washington, DC 20017
Attn: Dr. S. Heller, Dept of
Civil & Mech Engr.

2 Florida Atlantic University
Ocean Engineering Department
Boca Raton, FL 33432
Attn: Technical Library
Dr. S. Dunne

1 University of Hawaii
Department of Ocean Engineering
2565 The Mall
Honolulu, HI 96822
Attn: Dr. C. Bretschneider

1 Institute of Hydraulic Research
The University of Iowa
Iowa City, IA 52240
Attn: Library

4 Department of Ocean Engineering
Massachusetts Institute of
Technology
Cambridge, MA 02139
Attn: Department Library
Prof. P. Mandel
Prof. M. Abkowitz
Dr. J. Newman

2 St Anthony Falls Hydraulic Lab.
University of Minnesota
Mississippi River at 3rd Ave., S.E.
Minneapolis, MN 55414
Attn: Prof. E. Silberman
Dr. C. Song

3 Department of Naval Architecture
and Marine Engineering
University of Michigan
Ann Arbor, MI 48104
Attn: Library
Dr. T.F. Ogilvie
Prof. F. Hammitt

1 College of Engineering
University of Notre Dame
Notre Dame, IN 46556
Attn: Engineering Library

3 Davidson Laboratory
Stevens Institute of Technology
711 Hudson Street
Hoboken, NJ 07030
Attn: Library
Dr. J. Breslin
Dr. S. Tsakonas

2 Stanford University
Stanford, CA 94305
Attn: Engineering Library
Dr. R. Street

3 Webb Institute of Naval Architecture
Crescent Beach Road
Glen Cove, L.I., NY 11542
Attn: Library
Prof. E.V. Lewis
Prof. L.W. Ward

1 Applied Research Laboratory
P.O. Box 30
State College, PA 16801
Attn: Dr. B. Parkin, Director
Garfield Thomas Water Tunnel

1 Dr. Michael E. McCormick
Naval Systems Engineering Dept.
U.S. Naval Academy
Annapolis, MD 21402

1 Dr. Douglas E. Humphreys (Code 712)
Naval Coastal Systems Laboratory
Panama City, FL 32401